

Input-Output Data-Driven Representation: Non-Minimality and Stability

Joowon Lee, *Graduate Student Member, IEEE*, Nam Hoon Jo, *Member, IEEE*, Hyungbo Shim, *Senior Member, IEEE*, Florian Dörfler, *Senior Member, IEEE*, and Jinsung Kim, *Member, IEEE*

Abstract—Many recent data-driven control approaches for linear time-invariant systems are based on finite-horizon prediction of output trajectories using input-output data matrices. When applied recursively, this predictor forms a dynamic system representation. This data-driven representation is generally non-minimal, containing latent poles in addition to the system's original poles. In this article, we show that these latent poles are guaranteed to be stable through the use of the Moore-Penrose inverses of the data matrices, regardless of the system's stability and even in the presence of small noise in data. This result obviates the need to eliminate the latent poles through procedures that resort to low-rank approximation in data-driven control and analysis. It is then applied to construct a stabilizable and detectable realization from data, from which we design an output feedback linear quadratic regulator (LQR) controller. Furthermore, we extend this principle to data-driven inversion, enabling asymptotic unknown input estimation for minimum-phase systems.

Index Terms—Data-driven control, system identification, linear systems.

I. INTRODUCTION

IN recent years, there have been significant developments in data-driven control, particularly in methods for linear time-invariant (LTI) systems that use data matrices consisting of system trajectories [1]–[4], an idea that dates back to subspace methods [5], [6] and behavioral system theory [7]–[9]. Unlike classical approaches, these methods aim to bypass modeling of the system in terms of the transfer function or state-space representation, formulating controllers directly from the data matrices. Although these are categorized as *direct* approaches, as the counterpart of indirect approaches that involve system identification, they are often based on (non-classical) system representations that can be expressed by the data matrices.

This work was supported by the grant from Hyundai Motor Company's R&D Division and by the National Research Foundation of Korea(NRF) grant funded by the Korea government(MSIT) (No. RS-2022-00165417) & (No. 2022R1F1A1074838).

J. Lee and H. Shim are with ASRI, the Department of Electrical and Computer Engineering, Seoul National University, Seoul 08826, Korea (e-mail: jwlee@cddl.kr, hshim@snu.ac.kr).

N. H. Jo is with the Department of Electrical Engineering, Soongsil University, Seoul 06978, Korea (e-mail: nhjo@ssu.ac.kr).

F. Dörfler is with the Department of Information Technology and Electrical Engineering, ETH Zurich, Zurich 8092, Switzerland (e-mail: dorfler@ethz.ch).

J. Kim is with Advanced Vehicle Platform Division, Hyundai Motor Company, Seongnam 13529, Korea (e-mail: jinsung.kim@hyundai.com).

For example, data-enabled predictive control (DeePC) [1] in its basic form is equivalent to linear model predictive control where the LTI model equations at time $t \in \mathbb{Z}_{\geq 0}$ are replaced with the following formula:

$$Hg(t) := \begin{bmatrix} U_p \\ U_f \\ Y_p \end{bmatrix} g(t) = \begin{bmatrix} u(t-N:t-1) \\ u(t:t+M-1) \\ y(t-N:t-1) \end{bmatrix}, \quad (1a)$$

$$y(t:t+M-1) = Y_f g(t), \quad (1b)$$

where $u(t-N:t-1) = \text{col}(u(t-N), \dots, u(t-1)) \in \mathbb{R}^{mN}$ and $y(t-N:t-1) = \text{col}(y(t-N), \dots, y(t-1)) \in \mathbb{R}^{pN}$ are the system's past input-output trajectories, respectively, $u(t:t+M-1) \in \mathbb{R}^{mM}$ is the future input trajectory (the decision variable in predictive control), $y(t:t+M-1) \in \mathbb{R}^{pM}$ is the predicted output trajectory, and $g(t) \in \mathbb{R}^T$ is a solution to the linear equation (1a) given the matrix H determined by offline data. Specifically, the columns of the data matrices

$$\begin{bmatrix} U_p \\ U_f \end{bmatrix} \in \mathbb{R}^{m(N+M) \times T} \quad \text{and} \quad \begin{bmatrix} Y_p \\ Y_f \end{bmatrix} \in \mathbb{R}^{p(N+M) \times T} \quad (2)$$

are input and output trajectories of length $N+M$, respectively, and U_p , U_f , Y_p , and Y_f have mN , mM , pN , and pM rows, respectively. It is known that this prediction is consistent with a model-based prediction for any $g(t)$ satisfying (1a), if

$$\text{rank}(H) = m(N+M) + n \quad \text{with} \quad N \geq l, \quad (3)$$

where $n \in \mathbb{N}$ and $l \in \mathbb{N}$ are the minimal order and the lag of the system, respectively [10]. In other words, the formula (1) perfectly simulates the system. For details, see Section II-B.

Consider recursive one-step prediction by (1); that is, with $M = 1$, the current prediction $y(t)$ from (1b) is reused at the next time step as the most recent output in (1a). In this case, the formula (1) receives the current input $u(t)$ and produces the current output $y(t)$ based on its past behavior. From this viewpoint, the recursive use of (1) yields another system representation, similar to the state-space or ARX (autoregressive with exogenous inputs) model. Moreover, under the condition (3), the resulting input-output behavior of (1) coincides with that of the underlying system. This makes (1) a valid *data-driven representation* of the system—the topic of this article.

Despite the widespread use of (1) and its variations in data-driven control and analysis [1], [2], [4], [6], [8], [9], it has not been extensively studied as a dynamic system representation with recursive nature, providing a thorough stability analysis. In fact, the representation (1) contains *latent poles* in addition to the poles of the system, due to its non-minimality when

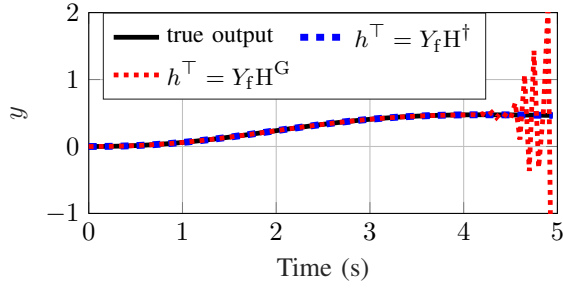


Fig. 1: The output of the system (the black solid line) and $y(t)$ of (4) when $h^\top = Y_f H^\dagger$ (the blue dashed line) and $h^\top = Y_f H^G$ with some randomly selected H^G (the red dotted line). More details on the simulation can be found in Section III-D.

$pN > n$ —a fundamental characteristic when input-output data are used instead of state measurements. To see this, for now consider a single-input single-output (SISO) system and noise-free data. Then, with $M = 1$, Y_f is a row vector that belongs to the row span of H , since the noise-free data are originated from an LTI system where the output is a linear combination of the input and the past N input-output pairs. Thus, with any $h \in \mathbb{R}^{2N+1}$ such that $Y_f = h^\top H$, (1) can be rewritten as

$$y(t) = h^\top \begin{bmatrix} u(t-N:t-1) \\ u(t) \\ y(t-N:t-1) \end{bmatrix}, \quad (4)$$

by substituting $h^\top H$ for Y_f in (1b) and using equality (1a).

Now it is clear that (4), or equivalently, (1) is a difference equation of inputs and outputs or an ARX model. By applying the z -transform to (4), we obtain a transfer function having N poles, which is identical to that of the underlying system after $N - n$ pole-zero cancellations. We refer to these $N - n$ poles, which would ideally be canceled, as the *latent poles*. In practice, these latent poles are not perfectly canceled due to numerical errors or noise in data, which is why unstable pole-zero cancellations should be avoided. Yet, to the best of our knowledge, it has not been addressed where the latent poles are located, whether an unstable pole-zero cancellation can occur, and if so, how their stability can be ensured.

We have observed that unstable pole-zero cancellations actually occur with an injudicious choice of h in (4), even when the underlying system is stable; Fig. 1 compares the output of a stable SISO system with those obtained by applying (4) recursively with $h^\top = Y_f H^\dagger$, where H^\dagger is the Moore-Penrose inverse of H , and $h^\top = Y_f H^G$, where H^G is some randomly selected generalized inverse¹ of H . As $N = 6$ and $n = 4$ in this simulation, there are two latent poles, and the red dotted line in Fig. 1 demonstrates that they can be unstable.

In this article, we show that the stability of every latent pole in the data-driven representation (4) is guaranteed when $h^\top = Y_f H^\dagger$, regardless of the underlying system's stability or the number of the latent poles. Adopting $Y_f H^\dagger$, known as the *subspace predictor* [6], [9], can be understood as choosing $g(t)$ of (1b) as the least-norm solution to (1a). This result directly

applies to multi-input single-output systems, and also extends to general multi-output systems with a slight modification. In such cases, we further show that the latent poles remain stable even in the presence of sufficiently small noise in data.

Stability analysis of the latent poles is crucial to data-driven control in several aspects. First, they are not easy to avoid or remove, particularly when the minimal order n or the lag l is unknown. For single-output systems, they can be avoided by setting $N = n$ as in [2], [11]. Ideally, n can be identified from the rank condition (3), which can be met by some persistency of excitation condition [7] on the input data without the exact knowledge of n and l (see Remark 1). However, when the data are noisy, the matrix H has higher rank in general. Although low-rank approximation of H can be conducted by observing its dominant singular values, this is essentially heuristic when the true rank is unknown. Moreover, for multi-output systems, the latent poles cannot be avoided in general by adjusting the parameter N alone, since (1) is non-minimal when $pN > n$. For this reason, prior works have assumed $n = pl$ [12], [13], or imposed other assumptions [14], both of which restrict the class of multi-output systems. Alternatively, in [15]–[19], the latent poles are removed subsequently by eliminating linearly dependent rows or portions from the data matrices; however, it is tedious and still requires low-rank approximation for noisy data matrices.

Secondly, for data-driven output feedback control, a common approach is to construct a non-minimal realization from data matrices, where the state consists of, or is derived from, the past N input-output pairs [2], [11]–[14], [17], [18]. The problem is that the presence of latent poles makes the non-minimal realization uncontrollable. To resolve this, they have been avoided or eliminated by the assumptions or methods in the previous paragraph. However, if the latent poles are stable and the non-minimal realization is stabilizable, then it would be still useful for output feedback control.

Indeed, it can be shown that such a non-minimal realization, constructed from the data-driven representation (4) with $h^\top = Y_f H^\dagger$, is always stabilizable for single-output systems due to the stability of every latent pole. For multi-output systems, we formulate a non-minimal realization by concatenating those of single-output systems, and provide a necessary and sufficient condition for its stabilizability. In addition, this non-minimal realization is always detectable by its structure.

As an application to data-driven control, we design an output feedback controller based on this non-minimal realization, given its stabilizability. This controller not only stabilizes the underlying system, but also produces the optimal solution to the classical model-based linear quadratic regulator (LQR) problem when its initial state is consistent with the system's actual initial input-output trajectory. Interestingly, it has been observed from simulation results that the controller's performance against online measurement noise tends to improve as N increases, that is, as the number of latent poles grows. This indicates that the latent poles can be regarded as beneficial, rather than as obstacles to be avoided.

Finally, it is essential to examine the stability of the latent poles for data-driven inversion [20]–[22], also referred to as data-driven unknown input estimation or reconstruction, which

¹ A^G is a generalized inverse of a matrix A if $AA^GA = A$. If a vector b belongs to the image of A , then $A^G b$ is a solution x to $Ax = b$ for any A^G .

estimates the system's input from the measured outputs using input-output data matrices. It has a variety of applications, including attack detection, internal model control [22], and data-driven disturbance observer (DD-DOB) [21], which estimates the input disturbance and rejects it simultaneously. Despite the recursive nature of previous data-driven inversion algorithms, where the current input estimate is reused to compute the next one, their stability has been overlooked [21], [22] or not fully understood [20]. In fact, it can be shown that these algorithms are data-driven representations of an L -delay inverse of the system, which accounts for the issues observed in practice for non-minimum phase systems. Moreover, latent poles may destabilize these algorithms even for minimum-phase systems.

In this context, we propose a modified data-driven inversion algorithm for SISO systems using the Moore-Penrose inverse of the data matrix whose latent poles are stable. This implies that the proposed algorithm is stable if and only if the system is of minimum-phase. The stability of this algorithm enables *asymptotic* data-driven input estimation, where the estimation error converges to zero for any initial guess of the unknown input trajectory. This property is particularly useful for DD-DOB since the initial disturbance is hardly known, while its original version [21] assumes its knowledge.

The rest of this article is organized as follows. Section II provides the problem formulation and preliminaries. In Section III, we analyze the stability of the data-driven representation (1) and present the main result on the stability guarantee of the latent poles. Section IV discusses applications of this result to data-driven output feedback control and presents an "output feedback" LQR controller as an example. Section V extends the analysis to data-driven inversion and introduces a novel input estimation algorithm together with its adaptation to DD-DOB. Finally, Section VI concludes the article.

A. Notations

The sets of real numbers, complex numbers, positive integers, and nonnegative integers are denoted by \mathbb{R} , \mathbb{C} , \mathbb{N} , and $\mathbb{Z}_{\geq 0}$, respectively. For $a_i \in \mathbb{R}^{m_i}$ with $i \in \{1, \dots, n\}$, we let $\text{col}(a_1, \dots, a_n) := [a_1^\top, \dots, a_n^\top]^\top$. For $n \in \mathbb{Z}_{\geq 0}$, P_n denotes the space of polynomials of degree no greater than n , and M_n denotes the set of monic polynomials of degree n . We write the Moore-Penrose inverse and a generalized inverse of a matrix A as A^\dagger and A^G , respectively. Let $I_n \in \mathbb{R}^{n \times n}$, $0_n \in \mathbb{R}^n$, and $0_{m \times n} \in \mathbb{R}^{m \times n}$ be the identity matrix, the zero vector, and the zero matrix, respectively, whose dimensions are omitted when clear from the context. The diagonal matrix whose i -th main diagonal element is a_i is denoted by $\text{diag}(a_1, \dots, a_n)$; it is also used for diagonal elements of rectangular matrices whose dimensions are clear. Let \otimes denote the Kronecker product. The real and the imaginary parts of $c \in \mathbb{C}$ are denoted by $\text{Re}(c)$ and $\text{Im}(c)$, respectively, which are defined element-wisely for vectors and matrices. For a matrix A , the nonzero minimum singular value and the maximum singular value are denoted by $\sigma_{\min}(A)$ and $\sigma_{\max}(A)$, respectively.

II. PROBLEM FORMULATION AND PRELIMINARIES

A. Problem Formulation

Consider a discrete-time LTI system with input $u(t) \in \mathbb{R}^m$, output $y(t) \in \mathbb{R}^p$, minimal order $n \in \mathbb{N}$, and lag $l \in \mathbb{N}$ (the observability index of a minimal realization). The system is described by a proper transfer function matrix

$$G(z) = \begin{bmatrix} G_1(z) \\ \vdots \\ G_p(z) \end{bmatrix},$$

where $G_i(z)$ is a $1 \times m$ nonzero transfer function matrix with minimal order $n_i \in \mathbb{N}$ for $i \in \{1, \dots, p\}$; this implies that each system $G_i(z)$ is non-autonomous and dynamic. Let

$$G_i(z) =: \frac{1}{D_i(z)} N_i(z), \quad i \in \{1, \dots, p\}, \quad (5)$$

where $D_i(z) \in M_{n_i}$ and $N_i(z) \in P_{n_i}^{1 \times m}$.

A state-space representation of the system is given by

$$\begin{aligned} x(t+1) &= Ax(t) + Bu(t), \\ y(t) &= Cx(t) + Du(t), \end{aligned} \quad (6)$$

where $x(t)$ is the state with dimension $n' \geq n$. Suppose that the system is unknown, i.e., all of $G(z)$, (A, B, C, D) , n , n' , and l are unknown, though both the minimal order and the lag have known upper bounds $\bar{n} \geq n$ and $\bar{l} \geq l$, respectively. We regard direct measurements of the state as unavailable.

Let $\mathcal{W}_k \subset \mathbb{R}^{(m+p)k}$ be the set of all length- k input-output trajectories of the system. With $M = 1$, i.e., for a single step prediction horizon, we construct the data matrices (2) so that each column of $\begin{bmatrix} H \\ Y_f \end{bmatrix}$, where H is defined in (1), belongs to \mathcal{W}_{N+1} . Here, the parameter N is chosen to be $N \geq \bar{l}$, and we assume that the data matrix satisfies the rank condition (3).

Remark 1. The rank condition (3) can be satisfied under some persistency of excitation assumption on the input data, which depends on the specific structure of the data matrices. For example, given a single data trajectory $\text{col}(u^d, y^d) \in \mathcal{W}_{T+N}$, let the data matrices (2) be Hankel matrices² $\mathcal{H}_{N+1}(u^d)$ and $\mathcal{H}_{N+1}(y^d)$, respectively. Then, the condition (3) holds if u^d is persistently exciting of order $\bar{n} + N + 1$, i.e., $\mathcal{H}_{\bar{n}+N+1}(u^d)$ has full row rank, by Willems' fundamental lemma [7] and [10]. Similar assumptions ensuring the condition (3) have also been explored with respect to the Page matrix [23] and the mosaic-Hankel matrix [24] (a generalization of the Hankel matrix for multiple data trajectories).

We define data matrices corresponding to the i -th output, as

$$Y_{p,i} := (I_N \otimes e_i^\top) Y_p, \quad Y_{f,i} := e_i^\top Y_f, \quad H_i := \begin{bmatrix} U_p \\ U_f \\ Y_{p,i} \end{bmatrix},$$

where $e_i \in \mathbb{R}^p$ is the unit vector whose i -th component is 1.

²For a signal $u = \text{col}(u_0, \dots, u_{T'-1}) \in \mathbb{R}^{mT'}$ and $L \in \mathbb{N}$ such that $L \leq T'$, the Hankel operator \mathcal{H}_L is defined by

$$\mathcal{H}_L(u) := \begin{bmatrix} u_0 & \cdots & u_{T'-L} \\ \vdots & \ddots & \vdots \\ u_{L-1} & \cdots & u_{T'-1} \end{bmatrix} \in \mathbb{R}^{mL \times (T'-L+1)}.$$

Henceforth, we consider the data-driven representation (1) with $M = 1$, and show that i) it contains latent poles (the poles aside from the system's original poles) that can be unstable, and ii) the stability of every latent pole is always guaranteed by employing the Moore-Penrose inverse of each H_i .

B. Preliminaries

This subsection illustrates how (1) exhibits the same input-output behavior as the system, being a valid system representation. The following proposition summarizes the results from [7], [8], [10] applied to (1).

Proposition 1. For $N \geq l$, $\text{image} \begin{bmatrix} H \\ Y_f \end{bmatrix} = \mathcal{W}_{N+M}$ if and only if (3) holds. Under this condition, given $u(t-N : t+M-1)$ and $y(t-N : t-1)$, $y(t : t+M-1)$ is uniquely determined by (1b) for any $g(t) \in \mathbb{R}^T$ satisfying (1a).

Proof. Since the system is LTI, $\text{image} \begin{bmatrix} H \\ Y_f \end{bmatrix} \subset \mathcal{W}_{N+M}$. By [7] and [10], $\dim(\mathcal{W}_{N+M}) = m(N+M) + n$, and thus the equality holds if and only if (3) holds. The rest of the proof directly follows from [8, Proposition 1]. \square

By Proposition 1, under the condition (3), (1) is well-defined if and only if $\text{col}(u(t-N : t-1), y(t-N : t-1)) \in \mathcal{W}_N$. It also states that (1) correctly predicts the system's future output trajectory $y(t : t+M-1)$, given the system's past input-output trajectory and the future input trajectory $u(t : t+M-1)$.

III. DATA-DRIVEN REPRESENTATION WITH STABLE LATENT POLES

We demonstrate how latent poles are generated by the data-driven representation (1), and show that their stability is always guaranteed by adopting the Moore-Penrose inverses of the data matrices and reformulating (1) as follows:

$$y_i(t) = Y_{f,i} H_i^\dagger \begin{bmatrix} u(t-N : t-1) \\ u(t) \\ y_i(t-N : t-1) \end{bmatrix}, \quad i \in \{1, \dots, p\}, \quad (7a)$$

$$y(t) = [y_1(t), \dots, y_p(t)]^\top. \quad (7b)$$

It is also analyzed how the latent poles of (7) are affected by noisy data, ensuring that they remain stable under sufficiently small noise. We begin with the case of single-output systems, and then present the result for the general multi-output case.

A. Single-Output Case

Let $p = 1$. As discussed in Section I, the data-driven representation (1) can be rewritten as (4) for any $h \in \mathbb{R}^{m(N+1)+N}$ satisfying $Y_f = h^\top H$. Such h always exists since the data are noise-free and the underlying system is LTI.

We first show the existence of latent poles from (4). Let

$$h = [\beta_0^\top, \dots, \beta_{N-1}^\top, \beta_N^\top, \alpha_0, \dots, \alpha_{N-1}]^\top, \quad (8)$$

where $\beta_k \in \mathbb{R}^m$ for $k \in \{0, 1, \dots, N\}$ and $\alpha_k \in \mathbb{R}$ for $k \in \{0, 1, \dots, N-1\}$. Since (1), and therefore (4) describes the

input-output behavior of the system, applying the z -transform to (4) yields the transfer function matrix $G(z)$ so that

$$\frac{1}{z^N - \sum_{k=0}^{N-1} \alpha_k z^k} \sum_{k=0}^N \beta_k^\top z^k = G(z) =: \frac{1}{D(z)} N(z), \quad (9)$$

where $D(z) \in M_n$ and $N(z) \in P_n^{1 \times m}$. Therefore, $N-n$ latent poles exist in (4), as stated by the following lemma.

Lemma 1. Under the condition (3), for any vector h in (8) satisfying $Y_f = h^\top H$, there exists $C(z) \in M_{N-n}$ such that

$$z^N - \sum_{k=0}^{N-1} \alpha_k z^k = C(z) D(z), \quad \sum_{k=0}^N \beta_k^\top z^k = C(z) N(z). \quad (10)$$

Conversely, for any $C(z) \in M_{N-n}$, the vector (8) constructed from (10) satisfies $Y_f = h^\top H$.

Proof. Given a vector h written as (8) satisfying $Y_f = h^\top H$, (9) holds by Proposition 1. Then, since there is no $\omega \in \mathbb{C}$ such that $D(\omega) = 0$ and $N(\omega) = 0_m^\top$, $D(z)$ (of degree n) divides $z^N - \sum_{k=0}^{N-1} \alpha_k z^k$ (of degree N), and thus (10) holds for some $C(z) \in M_{N-n}$. Conversely, given $C(z) \in M_{N-n}$, the vector (8) constructed from (10) satisfies $Y_f = h^\top H$ because the data obey the input-output relation described by $G(z)$. \square

Lemma 1 implies that the collection of $N-n$ latent poles, represented by the polynomial $C(z)$ in (10), is determined by the choice of solution h to the linear equation $Y_f = h^\top H$. It also shows that any monic polynomial $C(z)$ of degree $N-n$ corresponds to such h . For SISO systems, this means that the transfer function $G(z)$ with any possible combination of $N-n$ pole-zero cancellations can be obtained from (4). This is why unstable pole-zero cancellations can occur as shown in Fig. 1.

Now we show that every latent pole in (7), or equivalently, (4) with $h^\top = Y_f H^\dagger$ is always stable. To this end, we define a function Φ that maps h in (4) to $C(z)$ in (10), that is, $\Phi(h) := C(z)$. Thus, we aim to show that

$$C^*(z) := \Phi((Y_f H^\dagger)^\top)$$

is a Schur stable polynomial. We utilize the fact that $(Y_f H^\dagger)^\top$ is the least-norm solution to $Y_f = h^\top H$, i.e.,

$$(Y_f H^\dagger)^\top = \underset{h \in \mathbb{R}^{m(N+1)+N}}{\text{argmin}} \|h\|_2^2 \quad (11)$$

subject to $Y_f = h^\top H$.

As the function Φ is surjective onto M_{N-n} by Lemma 1 and is injective by definition, (11) can be rewritten as

$$C^*(z) = \underset{C(z) \in M_{N-n}}{\text{argmin}} \|\Phi^{-1}(C(z))\|_2^2. \quad (12)$$

To utilize (12), we introduce a new cost function; for $n \in \mathbb{N}$ and $\tau \in \mathbb{Z}_{\geq 0}$, $f_{n,\tau} : M_\tau \times M_n \times P_n^{1 \times m} \rightarrow \mathbb{R}$ is defined by

$$f_{n,\tau}(r(z), p(z), q(z)) := \left\| [\bar{q}_0^\top, \dots, \bar{q}_{n+\tau}^\top, \bar{p}_0, \dots, \bar{p}_{n+\tau-1}]^\top \right\|_2^2, \quad (13)$$

where

$$r(z)p(z) = z^{n+\tau} - \sum_{k=0}^{n+\tau-1} \bar{p}_k z^k, \quad r(z)q(z) = \sum_{k=0}^{n+\tau} \bar{q}_k^\top z^k,$$

so that $f_{n,N-n}(C(z), D(z), N(z)) = \|\Phi^{-1}(C(z))\|_2^2$. With this definition in hand, we rewrite (12) as

$$C^*(z) = \underset{C(z) \in M_{N-n}}{\operatorname{argmin}} f_{n,N-n}(C(z), D(z), N(z)). \quad (14)$$

It can be observed from (14) that the polynomial $C^*(z)$ is determined by the system $G(z)$ and the parameter N . In other words, under a fixed N , the latent poles of (7) are the same for any data satisfying the rank condition (3).

Next, we show that given $n \in \mathbb{N}$, $\tau \in \mathbb{Z}_{\geq 0}$, $p(z) \in M_n$, and $q(z) \in P_n^{1 \times m}$, any polynomial $r(z) \in M_\tau$ that minimizes the cost function (13) is Schur stable; then, the Schur stability of (14) is straightforward. As a first step, we consider the case when $\tau = 1$ and 2.

Lemma 2. *Given $n \in \mathbb{N}$, $p(z) \in M_n$, and $q(z) \in P_n^{1 \times m}$, the followings hold:*

1) *A solution $\lambda^* \in \mathbb{R}$ to*

$$\underset{\lambda \in \mathbb{R}}{\operatorname{minimize}} f_{n,1}(z + \lambda, p(z), q(z))$$

is unique and $|\lambda^| < 1$.*

2) *A solution $[\phi^*, \psi^*]^\top \in \mathbb{R}^2$ to*

$$\underset{[\phi, \psi]^\top \in \mathbb{R}^2}{\operatorname{minimize}} f_{n,2}(z^2 + \phi z + \psi, p(z), q(z))$$

is unique and $\psi^ < 1$.*

Proof. See the Appendix I. \square

Based on Lemma 2, we present the following lemma with respect to any $\tau \in \mathbb{N}$.

Lemma 3. *Given $n \in \mathbb{N}$, $p(z) \in M_n$, and $q(z) \in P_n^{1 \times m}$, any polynomial $r(z) \in M_\tau$ that minimizes (13) is Schur stable for all $\tau \in \mathbb{N}$.*

Proof. Given $\tau \in \mathbb{N}$, let $r^*(z) \in M_\tau$ minimize (13). Suppose that there exists a root $\lambda \in \mathbb{C}$ of $r^*(z)$ such that $|\lambda| \geq 1$. First, consider the case when $\lambda \in \mathbb{R}$. Then, $r^*(z)$ can be factorized as $r^*(z) = (z - \lambda)r_1(z)$, and by definition (13),

$$\begin{aligned} f_{n,\tau}(r^*(z), p(z), q(z)) \\ = f_{n+\tau-1,1}(z - \lambda, r_1(z)p(z), r_1(z)q(z)). \end{aligned} \quad (15)$$

However, by Lemma 2, the right hand side of (15) is strictly greater than when λ is replaced with some λ^* such that $|\lambda^*| < 1$. Thus, (13) has less value when $r(z) = (z - \lambda^*)r_1(z)$, which contradicts that $r^*(z)$ minimizes (13). Next, suppose $\lambda \notin \mathbb{R}$, which implies that $\tau > 1$. Then, the complex conjugate $\bar{\lambda}$ of λ is also a root of $r^*(z)$, and therefore $r^*(z)$ is factorized as $r^*(z) = (z - \lambda)(z - \bar{\lambda})r_2(z) =: (z^2 + \phi z + \psi)r_2(z)$, where $\psi^2 = |\lambda|^2 \geq 1$. The rest of the proof is analogous to that of the case when $\lambda \in \mathbb{R}$. \square

The analysis so far ensures that for single-output systems, every latent pole in the data-driven representation (7) is stable. In what follows, we extend this result to multi-output systems.

Remark 2. *For single-output systems, the data-driven representation (7) coincides with the subspace predictor [6], [9]. It can also be obtained directly from (1) by choosing $g(t)$ of (1b) as the least-norm solution to (1a), which is enforced by projection-based regularization schemes [25].*

B. General Result

For multi-output systems, the data-driven representation (1) can be reformulated as

$$y(t) = \begin{bmatrix} h_1^\top \\ \vdots \\ h_p^\top \end{bmatrix} \begin{bmatrix} u(t - N : t - 1) \\ u(t) \\ y(t - N : t - 1) \end{bmatrix}, \quad (16)$$

with any $h_i \in \mathbb{R}^{m(N+1)+pN}$ satisfying $Y_{f,i} = h_i^\top H$ for each i . As (4) in the single-output case, such h_i is non-unique for every i when $pN > n$ by the condition (3). This implies that the representation (16) is generally overparameterized (or non-minimal), which can be regarded as the fundamental cause of the emergence of latent poles.

In fact, (7) is a special case of (16) when each h_i^\top in (16) is constructed from $Y_{f,i}H_i^\dagger$ by appropriately inserting zeros; each $Y_{f,i}$ belongs to the row span of H_i as well as H , because the transfer function matrix $G_i(z)$ is well-defined so that the i -th output is a linear combination of the previous i -th outputs and the current and previous inputs. Therefore, (7) is also a valid representation of the system.

Now we introduce the main result; (7a) for each i represents each single-output system $G_i(z)$, having $N - n_i$ latent poles that are always stable. Recall that $G_i(z)$ has minimal order n_i and is written as (5).

Theorem 1. *Consider the data-driven representation (7). For each $i \in \{1, 2, \dots, p\}$, let*

$$Y_{f,i}H_i^\dagger = [b_{0,i}^\top, \dots, b_{N-1,i}^\top, b_{N,i}^\top, a_{0,i}, \dots, a_{N-1,i}], \quad (17)$$

where $a_{k,i} \in \mathbb{R}$ and $b_{k,i} \in \mathbb{R}^m$ for each k . Under the condition (3), there exists a Schur stable $C_i^(z) \in M_{N-n_i}$ such that*

$$z^N - \sum_{k=0}^{N-1} a_{k,i} z^k = C_i^*(z)D_i(z), \quad \sum_{k=0}^N b_{k,i}^\top z^k = C_i^*(z)N_i(z). \quad (18)$$

Furthermore, each $C_i^(z)$ is determined solely by $G_i(z)$ and N .*

Proof. Since (7) is a special case of (16) that is equivalent to (1), applying the z -transform to (7) yields the transfer function matrix $G(z)$ by Proposition 1. Then, for every $i \in \{1, \dots, p\}$,

$$\frac{1}{z^N - \sum_{k=0}^{N-1} a_{k,i} z^k} \sum_{k=0}^N b_{k,i}^\top z^k = G_i(z)$$

and thus (18) holds for some $C_i^*(z) \in M_{N-n_i}$, analogously to Lemma 1. Following the derivation in Section III-A,

$$C_i^*(z) = \underset{C(z) \in M_{N-n_i}}{\operatorname{argmin}} f_{n_i, N-n_i}(C(z), D_i(z), N_i(z)),$$

which shows that $C_i^*(z)$ is determined solely by $G_i(z)$ and N . In addition, by Lemma 3, $C_i^*(z)$ is a Schur stable polynomial, which concludes the proof. \square

We emphasize that the stability of every latent pole in (7) is guaranteed by Theorem 1, regardless of the stability of the system or the number of the latent poles, as long as the data satisfies the condition (3). Theorem 1 also states that the latent

poles depend only on the system and the parameter N , not on the particular choice of data.

Due to the presence of the latent poles, the stability of the underlying system is necessary but not sufficient in general for the stability of (16). However, the particular representation (7) with the Moore-Penrose inverses preserves the underlying system's stability by Theorem 1, since no unstable latent pole appears. Therefore, when applied recursively, (7) becomes a stable output predictor if and only if the system is stable; the predicted output asymptotically approaches the system's output even when the initial output trajectory of length N is not perfectly known, as stated by the following corollary.

Corollary 1. *Let $\hat{y}(t)$ be the predicted output by recursively applying (7). Then, under the condition (3), $\|y(t) - \hat{y}(t)\| \rightarrow 0$ as $t \rightarrow \infty$ for any initial prediction $\hat{y}(-N : -1) \in \mathbb{R}^{pN}$ if and only if the system is stable.*

Proof. For $i \in \{1, \dots, p\}$, define the i -th prediction error by $e_i^y(t) := y_i(t) - \hat{y}_i(t)$, where $\hat{y}_i(t)$ is the i -th element of $\hat{y}(t)$. Then, each $e_i^y(t)$ follows the dynamics of

$$e_i^y(t) = [a_{0,i} \quad a_{1,i} \quad \dots \quad a_{N-1,i}] e_i^y(t - N : t - 1), \quad (19)$$

which is stable if and only if $C_i^*(z)D_i(z)$ of (18) is Schur stable. Therefore, the dynamics of $y(t) - \hat{y}(t)$ is stable if and only if $C_i^*(z)D_i(z)$ is Schur stable for every $i \in \{1, \dots, p\}$, which holds if and only if $D_i(z)$ is Schur stable for every i by Theorem 1. This concludes the proof. \square

Remark 3. *It can be inferred from (16) that the data matrix H needs to have full row rank, i.e., $n = pN$ by (3), in order to avoid latent poles. The condition $n = pN$ for some $N \geq l$ can only be satisfied by a very restricted class of multi-output systems. This shows the difficulty of avoiding the latent poles, highlighting the importance of ensuring their stability.*

C. Effect of Noisy Data

Now we analyze the effect of noise in data on the stability of the data-driven representation (7). We consider a single-output system for simplicity, but the analysis in this subsection can be easily extended to the multi-output case.

Suppose that the representation (7) is implemented with the noisy data matrices

$$\tilde{H} = H + E, \quad \tilde{Y}_f = Y_f + e,$$

where E and e are output measurements noises. If $\tilde{Y}_f \tilde{H}^\dagger \rightarrow Y_f H^\dagger$ as both $E \rightarrow 0$ and $e \rightarrow 0$, then we can claim that, with sufficiently small noises, the poles of (7) with \tilde{Y}_f and \tilde{H} are not much different from those with Y_f and H . However, it does not hold in general that $\lim_{E \rightarrow 0} (H + E)^\dagger = H^\dagger$. While this property holds for the perturbation E that preserves the rank (i.e., $\text{rank}(H + E) = \text{rank}(H)$) [26], this cannot be expected for the random noise E .

Nevertheless, it is shown in this subsection that the property holds for the truncated Moore-Penrose inverse, which does not necessarily preserve the rank. Particularly, most numerical packages such as MATLAB and NumPy compute a truncated version of the Moore-Penrose inverse, since the non-truncated form is numerically unstable in the presence of small singular

values. In this regard, the above property holds “in practice,” as will be shown in Theorem 2.

Definition 1. *Let $A \in \mathbb{R}^{m \times n}$ have the singular value decomposition $U \Sigma V^\top$ where $\Sigma = \text{diag}(\sigma_1, \dots, \sigma_h)$ with $\sigma_1 \geq \sigma_2 \geq \dots \geq \sigma_h \geq 0$ ($h := \min\{m, n\}$). Then, the truncated Moore-Penrose inverse of A with tolerance $\tau > 0$ is defined by*

$$[A_\tau]^\dagger := V^\top \begin{bmatrix} \Sigma_\tau^{-1} & 0 \\ 0 & 0 \end{bmatrix} U,$$

where $\Sigma_\tau := \text{diag}(\sigma_1, \dots, \sigma_\kappa)$ with κ such that $\sigma_\kappa > \tau \geq \sigma_{\kappa+1}$ ($\sigma_{h+1} := 0$).

Note that in general, $\text{rank}(H^\dagger) \leq \text{rank}([\tilde{H}_\tau]^\dagger) \leq \text{rank}(\tilde{H}^\dagger)$ by definition, given a sufficiently small tolerance $\tau > 0$.

Now we consider (7) with

$$\tilde{Y}_f [\tilde{H}_\tau]^\dagger = [\tilde{b}_0^\top, \dots, \tilde{b}_{N-1}^\top, \tilde{b}_N^\top, \tilde{a}_0, \dots, \tilde{a}_{N-1}], \quad (20)$$

where $\tilde{b}_k \in \mathbb{R}^m$ and $\tilde{a}_k \in \mathbb{R}$ for each k . Then, the roots of $z^N - \sum_{k=0}^{N-1} \tilde{a}_k z^k$ are exactly the poles of (7) with (20).

Theorem 2. *Under the rank condition (3), let p_1, \dots, p_n be the roots of $D(z)$, and let q_1, \dots, q_{N-n} be the roots of $C^*(z)$. If $0 < \tau < \sigma_{\min}(H)$, then for any $\epsilon > 0$, there exists $\delta > 0$ such that*

$$z^N - \sum_{k=0}^{N-1} \tilde{a}_k z^k = \prod_{k=1}^n (z - \tilde{p}_k) \prod_{j=1}^{N-n} (z - \tilde{q}_j) \quad (21)$$

with $|\tilde{p}_k - p_k| < \epsilon$ for each k and $|\tilde{q}_j - q_j| < \epsilon$ for each j if $\|[E^\top, e^\top]\|_2 < \delta$.

Proof. The proof directly follows from Lemma 5 in the Appendix II and the fact that $D(z)C^*(z)$ and $z^N - \sum_{k=0}^{N-1} \tilde{a}_k z^k$ have the same degree, and is thus omitted. \square

Combining Theorems 1 and 2, it can be concluded that the latent poles in (7) from noisy data, i.e., \tilde{q}_j 's in (21) are stable under sufficiently small noise. Note that unlike the noise-free case, the latent poles \tilde{q}_j 's in (21) depend on data.

Remark 4. *Unlike computation of $[\tilde{H}_\tau]^\dagger$, low-rank approximation of \tilde{H} requires that the approximated \tilde{H} has the same rank as H . When the desired rank is unknown, such approximation often involves a heuristic procedure of inspecting the relatively dominant singular values of a given matrix, as done in [6], [17]. On the contrary, our analysis of (7) with $\tilde{Y}_f [\tilde{H}_\tau]^\dagger$ holds without relying on such a heuristic procedure or requiring the knowledge of the system's minimal order n to know $\text{rank}(H)$.*

Remark 5. *When the measurement noise has zero mean, its effect on (7) can be mitigated in practice by averaging $\tilde{Y}_f [\tilde{H}_\tau]^\dagger$ across multiple data trajectories, since $Y_f H^\dagger$ itself is invariant to the specific data by Theorem 1. Although one can construct a large mosaic-Hankel matrix from multiple data trajectories [24], it is generally more computationally efficient to compute the Moore-Penrose inverses of the individual Hankel matrices constructed from each trajectory, rather than that of a single large mosaic-Hankel matrix. However, this averaging method requires that each data trajectory satisfy the condition (3) in the absence of noise, under a fixed N . Note also that it yields a biased predictor of $Y_f H^\dagger$ due to the noise in \tilde{H} .*

D. Numerical Examples

We provide numerical examples that demonstrate the stability of the latent poles in the data-driven representation (7).

1) Stable System: We describe how the result of Fig. 1 is obtained. Consider a mass-spring-damper system of two point masses that are connected sequentially by springs and dampers between two walls. The system is written as [27]

$$\begin{aligned} m_1 \ddot{p}_1 &= -(k_0 + k_1)p_1 - (d_0 + d_1)\dot{p}_1 + k_1 p_2 \\ &\quad + d_1 \dot{p}_2 + u, \\ m_2 \ddot{p}_2 &= k_1 p_1 + d_1 \dot{p}_1 - (k_1 + k_2)p_2 - (d_1 + d_2)\dot{p}_2, \\ y &= p_1, \end{aligned} \quad (22)$$

and is stable. Let the parameters of (22) be $m_1 = 10$, $m_2 = 9$, $k_0 = 0.5$, $k_1 = 9$, $k_2 = 0.1$, $d_0 = 0.2$, $d_1 = 1.8$, and $d_2 = 0.3$. It is discretized under the sampling period 0.05 s, and its minimal order n is 4.

We collected input-output data u^d and y^d of length 100 and constructed data Hankel matrices with $N = 6$ that satisfy the condition (3), as described in Remark 1. The representation (4) is implemented for two cases, when $h^\top = Y_f H^\dagger$ and when $h^\top = Y_f H^G$ with a randomly generated³ generalized inverse H^G . Given the input $u(t) = 2 \sin(0.05t)$, Fig. 1 compares the outputs of (4) for these two cases with the true output of the system when the initial state is $(p_1, p_2, \dot{p}_1, \dot{p}_2) = (0, 0.1, 0, 0)$. For both cases, it is assumed that the initial trajectory of the true output is known for $t \in [0, N)$.

As $N - n = 2$, there are two latent poles in (4). When $h^\top = Y_f H^\dagger$, they are located at $-0.6669 \pm 0.4714i$, inside the unit circle. On the other hand, they are at $-1.3667 \pm 0.5788i$ when $h^\top = Y_f H^G$ with our randomly generated H^G . Ideally, the behavior of (4) should be identical to that of the system, as long as h satisfies $Y_f = h^\top H$. However, since there is no perfect pole-zero cancellation in reality, numerical errors are amplified by the unstable latent poles, as depicted in Fig. 1.

2) Unstable System: We validate the stability of the latent poles in (7) when the system is unstable, while varying their number and injecting noise into the data. Consider an inverted pendulum on a cart, which is written as

$$\begin{aligned} (I + ml^2) \ddot{\theta} - mgl\theta &= ml\ddot{x}, \\ (M + m) \ddot{x} + b\dot{x} - ml\ddot{\theta} &= u, \quad y = x + 2l\theta \end{aligned} \quad (23)$$

after linearization [28]. The parameters in (23) are set as $M = 0.5$, $m = 0.2$, $b = 0.1$, $l = 0.3$, $I = 0.006$, and $g = 9.81$. The system (23) is discretized under the sampling period 0.05 s. Note that it is unstable and has minimal order $n = 4$.

We collected 10 pairs of input-output data u^d and y^d such that $\text{col}(u^d, y^d) \in \mathcal{W}_{50}$ and the condition (3) holds for all $N \in [4, 16]$ when the matrices of (2) are $\mathcal{H}_{N+1}(u^d)$ and $\mathcal{H}_{N+1}(y^d)$, respectively. Using the method of Remark 5, $Y_f H^\dagger$ is averaged

³When a matrix A is written in the singular value decomposition, its (non-unique) generalized inverse can be written as

$$A = U \begin{bmatrix} \Sigma & 0 \\ 0 & 0 \end{bmatrix} V^\top, \quad A^G = V \begin{bmatrix} \Sigma^{-1} & X \\ Y & Z \end{bmatrix} U^\top$$

where U and V are orthogonal, Σ is diagonal with nonzero singular values, and X , Y , and Z are any matrices of suitable sizes. We have randomly generated these X , Y , and Z to obtain a generalized inverse.

across the 10 input-output data trajectories. We also collected the same data in the presence of output measurement noise, which follows a zero-mean Gaussian distribution with standard deviation $\sigma = 0.01$, and obtained $\tilde{Y}_f[\tilde{H}_\tau]^\dagger$ in the same manner. For the computation of the truncated Moore-Penrose inverses, the tolerance τ is not manually set and the function `pinv` in MATLAB is used under the default setting.

Fig. 2 shows that all the latent poles of (7) are stable for different values of N . Specifically, in the noise-free case, the latent poles are canceled by the corresponding zeros, while the remaining poles and zeros coincide with those of the system, therefore overlapped and invisible in Fig. 2. The latent poles are also inside the unit circle in the noisy case, but they do not overlap with zeros, and the rest of the poles and zeros deviate from those of the system.

Unlike the denominator (21) of the noisy representation's transfer function, the numerator $\sum_{k=0}^N \tilde{b}_k z^k$ can have different degree from $C^*(z)N(z)$ because noise may create a nonzero higher-order coefficient; in this example, the latter has degree $N - 1$, however, the former has degree N with a small leading coefficient due to noise. This implies that the representation (7) has one more zero in the noisy case than in the noise-free case. Nevertheless, under sufficiently small noise, $\sum_{k=0}^N \tilde{b}_k z^k$ has one distinctive large root and the rest of the roots are located near those of $C^*(z)N(z)$, by the principle of [29, Lemma 1]. This additional zero does not appear in Fig. 2 due to its large magnitude, and can be easily removed in practice.

IV. APPLICATION TO DATA-DRIVEN OUTPUT FEEDBACK CONTROL

A. Non-Minimal State-Space Realization

We discuss how the data-driven representation (7), which is guaranteed to contain only stable latent poles, can be used for data-driven output feedback control. To this end, we formulate a non-minimal state-space realization, where the state variable $\chi(t) \in \mathbb{R}^{pN(m+1)}$ consists of the past inputs and outputs:

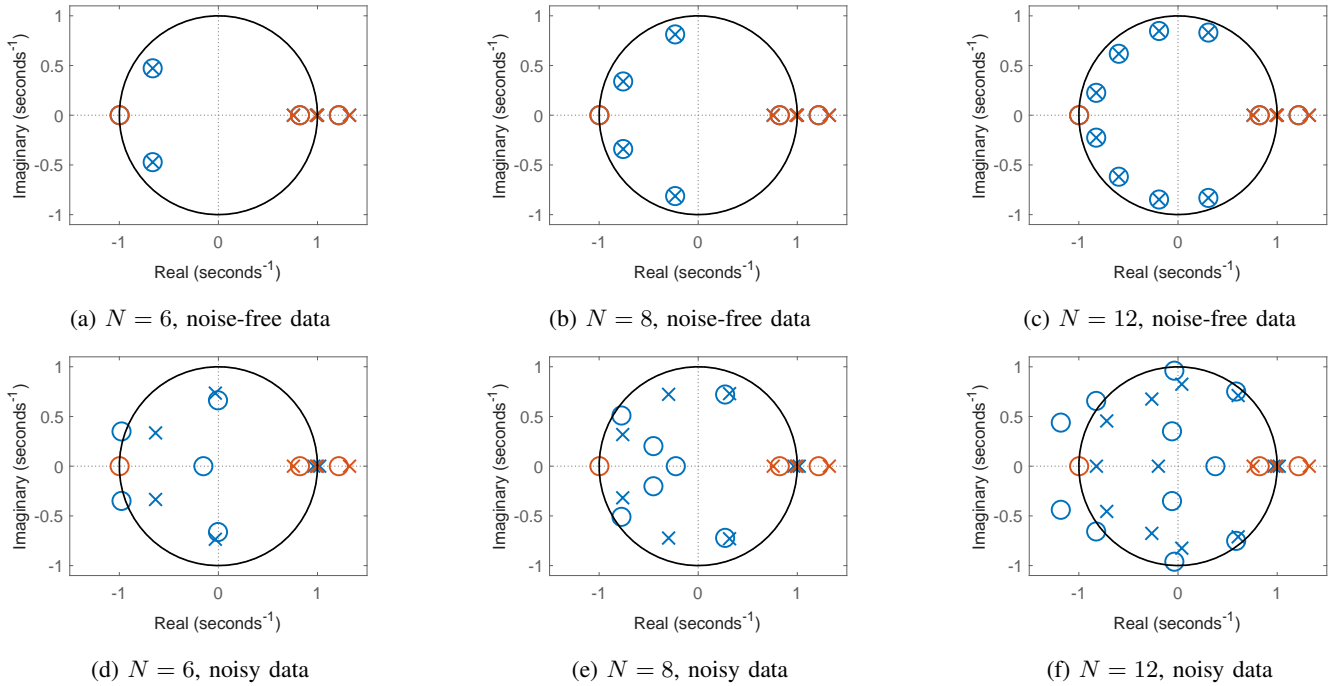
$$\chi(t) := \begin{bmatrix} \chi_1(t) \\ \vdots \\ \chi_p(t) \end{bmatrix}, \quad \chi_i(t) := \begin{bmatrix} y_i(t - N : t - 1) \\ u(t - N : t - 1) \end{bmatrix}. \quad (24)$$

With this state variable, the data-driven representation (7) can be equivalently written as

$$\begin{aligned} \chi(t+1) &= \mathcal{A}\chi(t) + \mathcal{B}u(t), \\ y(t) &= \mathcal{C}\chi(t) + \mathcal{D}u(t), \end{aligned} \quad (25)$$

where the matrices are defined using (17), by

$$(\mathcal{A}, \mathcal{B}, \mathcal{C}, \mathcal{D}) := \left(\begin{bmatrix} \mathcal{A}_1 & & \\ & \ddots & \\ & & \mathcal{A}_p \end{bmatrix}, \begin{bmatrix} \mathcal{B}_1 \\ \vdots \\ \mathcal{B}_p \end{bmatrix}, \begin{bmatrix} \mathcal{C}_1 & & \\ & \ddots & \\ & & \mathcal{C}_p \end{bmatrix}, \begin{bmatrix} \mathcal{D}_1 \\ \vdots \\ \mathcal{D}_p \end{bmatrix} \right)$$


$$\left[\begin{array}{c|c} \mathcal{A}_i & \mathcal{B}_i \\ \hline \mathcal{C}_i & \mathcal{D}_i \end{array} \right] := \left[\begin{array}{cccc|cccc} 0 & 1 & & & & & & 0_m^\top \\ \vdots & & \ddots & & & & & \vdots \\ 0 & & & 1 & & & & 0_m^\top \\ a_{0,i} & a_{1,i} & \cdots & a_{N-1,i} & b_{0,i}^\top & b_{1,i}^\top & \cdots & b_{N-1,i}^\top \\ & & & & 0_{m \times m} & I_m & & b_{N,i}^\top \\ & & & & \vdots & & \ddots & \vdots \\ & & & & 0_{m \times m} & & & I_m \\ & & & & 0_{m \times m} & & \cdots & 0_{m \times m} \\ \hline a_{0,i} & a_{1,i} & \cdots & a_{N-1,i} & b_{0,i}^\top & b_{1,i}^\top & \cdots & b_{N-1,i}^\top \end{array} \right]$$

Proof. To avoid the trivial case, suppose that $(\mathcal{C}, \mathcal{A})$ is unobservable. Then, there exist $\lambda \in \mathbb{C}$ and a nonzero vector $\xi = \text{col}(\xi_1, \dots, \xi_p) \in \mathbb{R}^{pN(m+1)}$ ($\xi_i \in \mathbb{R}^{N(m+1)}$ for each i) such that $\mathcal{C}\xi = 0_p$ and $\mathcal{A}\xi = \lambda\xi$. This implies that there is a nonzero ξ_i such that $\mathcal{C}_i\xi_i = 0$ and $\mathcal{A}_i\xi_i = \lambda\xi_i$. Let us write $\xi_i = [v_{0,i}, \dots, v_{N-1,i}, w_{0,i}^\top, \dots, w_{N-1,i}^\top]^\top$, where $v_{j,i} \in \mathbb{R}$

$$\text{and } \sum_{k=1}^p \xi_k^\top \mathcal{B}_k = 0_m^\top. \quad (29)$$

Due to the structure of $(\mathcal{A}, \mathcal{B})$, (28) is equivalent to

$$\begin{aligned} a_{0,i}v_{N-1,i} &= \lambda v_{0,i}, \\ v_{j-1,i} + a_{j,i}v_{N-1,i} &= \lambda v_{j,i}, \quad j \in \{1, \dots, N-1\}, \end{aligned} \quad (30)$$

$$\begin{aligned} v_{N-1,i}b_{0,i} &= \lambda w_{0,i}, \\ v_{N-1,i}b_{j,i} + w_{j-1,i} &= \lambda w_{j,i}, \quad j \in \{1, \dots, N-1\}, \end{aligned} \quad (31)$$

and (29) is equivalent to

$$\sum_{k=1}^p v_{N-1,k}b_{N,k} + w_{N-1,k} = 0_m. \quad (32)$$

Note that (30) implies

$$v_{N-1,i}D_i^*(\lambda) = 0, \quad (33)$$

and (31) implies

$$v_{N-1,i} \sum_{k=0}^{N-1} \lambda^k b_{k,i} = \lambda^N w_{N-1,i}. \quad (34)$$

Finally, (32) and (34) imply

$$\sum_{k=1}^p v_{N-1,k}N_k^*(\lambda) = 0_m^\top. \quad (35)$$

(Sufficiency:) To avoid the trivial case, suppose that $(\mathcal{A}, \mathcal{B})$ is uncontrollable so that there exist λ and a nonzero ξ such that (27) holds. If $v_{N-1,i} = 0$ for all i , then ξ should be zero by (30) and (31). If $v_{N-1,i} \neq 0$ for some i , then (33) implies $D_i^*(\lambda) = 0$ for such i . Then, (35) becomes

$$\sum_{\{i: D_i^*(\lambda) = 0\}} v_{N-1,i}N_i^*(\lambda) = 0_m^\top, \quad (36)$$

which implies $|\lambda| < 1$ by the assumption. (Necessity:) Suppose that there exists $\lambda \in \mathbb{C}$ such that $|\lambda| \geq 1$ and the set (26) is linearly dependent. This means that for such λ , there exists a nonzero $v_{N-1,i}$ such that (36) holds. With such λ and $v_{N-1,i}$, (30) and (31) yield a nonzero ξ_i , and therefore (27) holds with a nonzero ξ and $|\lambda| \geq 1$, concluding the proof. \square

Remark 6. The necessary and sufficient condition of Proposition 3 can be checked on data, from $Y_{f,i}H_i^\top$'s, by the definitions of $D_i^*(z)$'s and $N_i^*(z)$'s. Moreover, it suffices to inspect the set (26) only for λ 's such that $D_i^*(\lambda) = 0$ for more than one i 's; if there is no such i , then the set (26) is empty and hence is linearly independent. If there is only one such i , then the set (26) is also linearly independent, since $N_i^*(\lambda) = C_i^*(\lambda)N_i(\lambda)$ is nonzero because $C_i^*(\lambda) \neq 0$ for $|\lambda| \geq 1$ (Theorem 1) and $N_i(\lambda) \neq 0_m^\top$ when $D_i(\lambda) = 0$.

In what follows, we provide sufficient conditions for the stabilizability of (25) that are pure properties of the system, based on the Schur stability of $C_i^*(z)$'s.

Corollary 2. Under the condition (3), the pair $(\mathcal{A}, \mathcal{B})$ of (25) is stabilizable if either of the following conditions holds:

- 1) $p = 1$.
- 2) The set $\{N_i(\lambda)^\top : i \text{ such that } D_i(\lambda) = 0\}$ is linearly independent over \mathbb{C} for all $\lambda \in \mathbb{C}$ such that $|\lambda| \geq 1$.

Proof. When $p = 1$, the set (26) is a singleton of a nonzero vector for any $\lambda \in \mathbb{C}$ such that $|\lambda| \geq 1$, since $C^*(\lambda)N(\lambda) \neq 0_m^\top$

because $N(\lambda) \neq 0_m^\top$ when $D(\lambda) = 0$, and $C^*(\lambda) \neq 0$ as $C^*(z)$ is a Schur stable polynomial by Theorem 1.

Now suppose that the condition 2) holds. Given $\lambda \in \mathbb{C}$ such that $|\lambda| \geq 1$, let

$$\sum_{\{i: D_i^*(\lambda) = 0\}} \omega_i [\text{Re}(N_i^*(\lambda)), \text{Im}(N_i^*(\lambda))]^\top = 0_{2m}.$$

for some $\omega_i \in \mathbb{R}$. Since $C_i^*(\lambda) \neq 0$ for every i by Theorem 1,

$$\sum_{\{i: D_i(\lambda) = 0\}} \omega_i N_i^*(\lambda) = \sum_{\{i: D_i(\lambda) = 0\}} \omega_i C_i^*(\lambda)N_i(\lambda) = 0_m^\top,$$

which implies that $\omega_i C_i^*(\lambda) = 0$ for all i such that $D_i(\lambda) = 0$. Again, $C_i^*(\lambda) \neq 0$ by Theorem 1 and thus $\omega_i = 0$, concluding the proof by Proposition 3. \square

Corollary 2 specifies a class of systems where the realization (25) from data is always stabilizable, which includes all single-output systems. The following example presents a multi-output system that satisfies condition 2) of Corollary 2.

Example 1. Consider

$$G(z) = \begin{bmatrix} \frac{1}{z-2} & \frac{1}{z-3} \\ \frac{1}{z} & \frac{1}{z-2} \end{bmatrix},$$

where $D_1(z) = (z-2)(z-3)$, $N_1(z) = [z-3, z-2]$, $D_2(z) = z(z-2)$, and $N_2(z) = [z-2, z]$. For $\lambda = 2$, the set $\{N_i(2)^\top : i = 1, 2\} = \{[-1, 0]^\top, [0, 2]^\top\}$ is linearly independent (over \mathbb{C}). Thus, by Corollary 2, $(\mathcal{A}, \mathcal{B})$ is stabilizable. \square

B. Design of Output Feedback LQR Controller

Given that the realization (25) is stabilizable, which largely owes to the stability of the latent poles, one can design a data-driven output feedback controller directly from (25); this does not require additional assumptions or measures to construct a controllable realization from data. As an example, we design an output feedback LQR controller from (25).

Consider the following LQR problem with respect to (6):

$$\begin{aligned} &\text{minimize}_{u[0], u[1], \dots} \sum_{k=0}^{\infty} y[k]^\top Q y[k] + u[k]^\top R u[k] \\ &\text{subject to } x[k+1] = Ax[k] + Bu[k], \quad y[k] = Cx[k], \\ &\quad x[0] = x(0), \end{aligned} \quad (37)$$

given positive definite matrices $Q \in \mathbb{R}^{p \times p}$ and $R \in \mathbb{R}^{m \times m}$. In this subsection, we assume that $D = 0$, (A, B) is stabilizable, and (C, A) is detectable. Thus, the problem (37) has a unique optimal solution [30] since $(Q^{1/2}C, A)$ is detectable.

The problem (37) can be alternatively written as

$$\begin{aligned} &\text{minimize}_{u[0], u[1], \dots} \sum_{k=0}^{\infty} y[k]^\top Q y[k] + u[k]^\top R u[k] \\ &\text{subject to } \chi[k+1] = \mathcal{A}\chi[k] + \mathcal{B}u[k], \quad y[k] = C\chi[k], \\ &\quad \chi[0] = \chi(0), \end{aligned} \quad (38)$$

since (25) is a non-minimal realization of the system and $\chi(0)$, defined by (24), consists of the system's initial N input-output pairs that yield $x(0)$. Due to this equivalence, the problem (38) also has a unique optimal solution. Note that $D = 0$ because $b_{N,i} = 0_m$ for all $i \in \{1, \dots, p\}$ by $D = 0$.

Assume that the pair $(\mathcal{A}, \mathcal{B})$ is stabilizable, i.e., the condition of Proposition 3 is satisfied. Recall that $(\mathcal{C}, \mathcal{A})$ is always detectable by Proposition 2. Then, there exists a unique positive semidefinite solution \mathcal{P} to the algebraic Riccati equation

$$\mathcal{P} = \mathcal{A}^\top \mathcal{P} \mathcal{A} + \mathcal{C}^\top \mathcal{Q} \mathcal{C} - \mathcal{A}^\top \mathcal{P} \mathcal{B} (\mathcal{B}^\top \mathcal{P} \mathcal{B} + R)^{-1} \mathcal{B}^\top \mathcal{P} \mathcal{A},$$

and with

$$\mathcal{K} := (\mathcal{B}^\top \mathcal{P} \mathcal{B} + R)^{-1} \mathcal{B}^\top \mathcal{P} \mathcal{A},$$

$\mathcal{A} - \mathcal{B}\mathcal{K}$ is Schur stable [30].

Now we present a data-driven output feedback controller as

$$\begin{aligned} \hat{\chi}(t+1) &= \mathcal{F}\hat{\chi}(t) + \mathcal{G}y(t), \\ u(t) &= -\mathcal{K}\hat{\chi}(t), \end{aligned} \quad (39)$$

where $\hat{\chi}(t) \in \mathbb{R}^{pN(m+1)}$ is the state and

$$\mathcal{G} := I_p \otimes \begin{bmatrix} 0_{N-1} \\ 1 \\ 0_{mN} \end{bmatrix}, \quad \mathcal{F} := \mathcal{A} - \mathcal{G}\mathcal{C} - \mathcal{B}\mathcal{K}.$$

Note that $\mathcal{A} - \mathcal{G}\mathcal{C}$ is exactly \mathcal{A} where all $a_{k,i}$'s and $b_{k,i}^\top$'s are replaced with zeros, and therefore is nilpotent. As shown by the following theorem, the controller (39) stabilizes the system (6), and also yields the optimal solution to the LQR problem (37) when its initial state consists of the system's initial input-output trajectory, i.e., when $\hat{\chi}(0) = \chi(0)$.

Theorem 3. *Under the condition (3) and the stabilizability of the pair $(\mathcal{A}, \mathcal{B})$, the controller (39) achieves the followings:*

- 1) *The closed-loop system (6) with (39) is stable.*
- 2) *Let the optimal solution to (37) be $u^*[0], u^*[1], \dots$. If $\hat{\chi}(0) = \chi(0)$, then $u(t) = u^*[t]$ for all $t \in \mathbb{Z}_{\geq 0}$.*

Proof. The characteristic polynomial of the closed-loop system (6) with (39) satisfies

$$\begin{aligned} \det \left(\begin{bmatrix} zI - \mathcal{A} & \mathcal{B}\mathcal{K} \\ -\mathcal{G}\mathcal{C} & zI - \mathcal{F} \end{bmatrix} \right) \\ = \det(zI - \mathcal{A}) \det(zI - \mathcal{F} + \mathcal{G}\mathcal{C}(zI - \mathcal{A})^{-1} \mathcal{B}\mathcal{K}) \\ = \det(zI - \mathcal{A}) \det(zI - \mathcal{F} + \mathcal{G}\mathcal{C}(zI - \mathcal{A})^{-1} \mathcal{B}\mathcal{K}) \\ = \frac{\det(zI - \mathcal{A})}{\det(zI - \mathcal{A})} \det \left(\begin{bmatrix} zI - \mathcal{A} & \mathcal{B}\mathcal{K} \\ -\mathcal{G}\mathcal{C} & zI - \mathcal{F} \end{bmatrix} \right), \end{aligned} \quad (40)$$

where the second equality comes from the fact that (25) and (6) have the same transfer function matrices. The closed-loop system (25) in feedback with (39) can be transformed into

$$\begin{aligned} e_\chi(t+1) &= (\mathcal{A} - \mathcal{G}\mathcal{C}) e_\chi(t), \\ \chi(t+1) &= (\mathcal{A} - \mathcal{B}\mathcal{K}) \chi(t) + \mathcal{B}\mathcal{K} e_\chi(t), \end{aligned}$$

where $e_\chi(t) := \chi(t) - \hat{\chi}(t)$. Then, (40) equals

$$\frac{\det(zI - \mathcal{A})}{\det(zI - \mathcal{A})} \det(zI - (\mathcal{A} - \mathcal{B}\mathcal{K})) \det(zI - (\mathcal{A} - \mathcal{G}\mathcal{C})),$$

and therefore is Schur stable. This is because $\mathcal{A} - \mathcal{B}\mathcal{K}$ is Schur stable, every eigenvalue of $\mathcal{A} - \mathcal{G}\mathcal{C}$ is at the origin, and lastly every unstable root of $\det(zI - \mathcal{A})$, that is a controllable and observable mode of (6), is a root of $\det(zI - \mathcal{A})$.

The optimal solution to (37), or equivalently, (38) is $u^*[k] = -\mathcal{K}\chi[k]$ for $k \in \mathbb{Z}_{\geq 0}$ when $\chi[0] = \chi(0)$. Due to the structure of (39), $\hat{\chi}(t) = \chi(t)$ for all $t \in \mathbb{Z}_{\geq 0}$ if $\hat{\chi}(0) = \chi(0)$, which implies that $u(t) = u^*[t]$ for all $t \in \mathbb{Z}_{\geq 0}$. \square

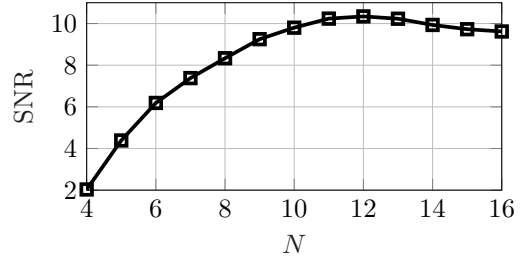


Fig. 3: Average SNR (defined by (41)) across the 10 input-output trajectories by varying N .

C. Simulation Results

We provide simulation results that demonstrate the performance of the proposed controller (39), with respect to a SISO and MIMO system, and discuss the effect of the parameter N .

1) SISO system: The linearized inverted pendulum (23) of Section III-D.2 is considered under the same setting. The data are collected in the same way as well, except that the output measurement noise follows a Gaussian distribution with zero mean and standard deviation $\sigma = 10^{-4}$. We define the signal-to-noise ratio (SNR) by

$$\text{SNR} := 10 \log_{10} \sigma_{\min} \left(\begin{bmatrix} H \\ Y_f \end{bmatrix} \right) - 10 \log_{10} \sigma_{\max} \left(\begin{bmatrix} E \\ e \end{bmatrix} \right). \quad (41)$$

The resulting SNR, which varies by N , is plotted in Fig. 3.

The weighting parameters of the LQR problem (37) are set as $Q = 100$ and $R = 1$. The controller (39) is implemented from both the noise-free and noisy data for each $N \in [4, 16]$. Fig. 4 shows the output of the system with the controller (39) when there is online output measurement noise that follows a zero-mean Gaussian distribution with standard deviation $\sigma = 10^{-3}$. The initial conditions were $(x, \dot{x}, \theta, \dot{\theta}) = (1, 0, 0, 0)$ and $\hat{\chi}(0) = [1, \dots, 1, 0_N^\top]^\top$. In this case, $\hat{\chi}(0) = \chi(0)$, and thus by Theorem 3, the controllers (39) with different values of N result in the same response without online noise. Meanwhile, the controllers from noisy data with $N = 4$ and 5 could not stabilize the system (23).

Fig. 4 shows that, as N increases, the performance of the controller (39) under online measurement noise improves. To see it clearly, we consider the closed-loop system of (6) with (39) from noise-free data, written as

$$\begin{aligned} \begin{bmatrix} x(t+1) \\ \hat{\chi}(t+1) \end{bmatrix} &= \begin{bmatrix} \mathcal{A} & -\mathcal{B}\mathcal{K} \\ \mathcal{G}\mathcal{C} & \mathcal{F} \end{bmatrix} \begin{bmatrix} x(t) \\ \hat{\chi}(t) \end{bmatrix} + \begin{bmatrix} 0 \\ \mathcal{G} \end{bmatrix} w(t), \\ z(t) &= \begin{bmatrix} Q^{1/2}C & 0 \\ 0 & R^{1/2}\mathcal{K} \end{bmatrix} \begin{bmatrix} x(t) \\ \hat{\chi}(t) \end{bmatrix}, \end{aligned} \quad (42)$$

where $w(t) \in \mathbb{R}^p$ is the external input representing the output measurement noise and $z(t) \in \mathbb{R}^{p+m}$ is the output whose l^2 -norm is the cost of the LQR problem (37). Let $\mathcal{T}_{wz}(z)$ denote the transfer function matrix of (42). Then, as shown in Fig. 5, the \mathcal{H}_2 norm of $\mathcal{T}_{wz}(z)$ decreases as N increases.

2) MIMO system: Let us consider a submarine longitudinal model at constant speed [31], written as

$$\dot{x} = A_c x + B_c u, \quad y = C_c x, \quad (43)$$

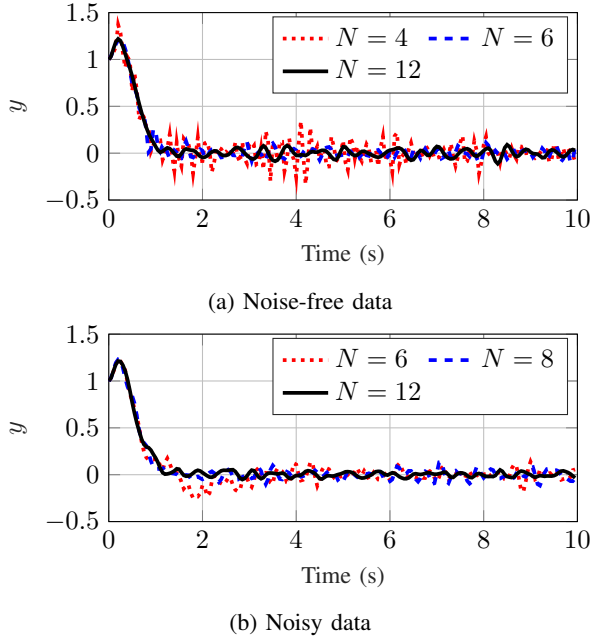


Fig. 4: Output of the system (23) with the controller (39) under online output measurement noise.

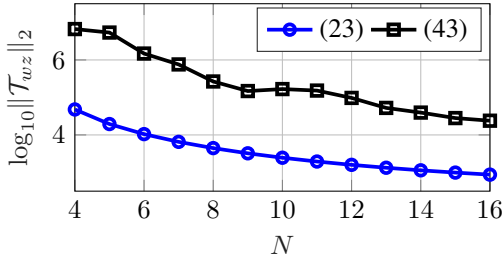


Fig. 5: \mathcal{H}_2 norm of the closed-loop system (42) with respect to the system (23) (the blue circle-marked line) and (43) (the black square-marked line) by varying N .

where $x \in \mathbb{R}^4$ is the state, $u \in \mathbb{R}^2$ is the input, $y \in \mathbb{R}^2$ is the output, and the matrices are defined by

$$A_c := \begin{bmatrix} -0.0123v & 0.29029v & 0 & 0.000475v \\ 0.000554v & -0.02979v & 0 & -0.001817v \\ 1 & 0 & 0 & -v \\ 0 & 1 & 0 & 0 \end{bmatrix},$$

$$B_c := v^2 \begin{bmatrix} -0.000791 & -0.002399 \\ 0.00018178 & -0.000233 \\ 0 & 0 \\ 0 & 0 \end{bmatrix}, C_c := \begin{bmatrix} 0 & 0 & 1 & 0 \\ 0 & 0 & 0 & 1 \end{bmatrix},$$

with submarine speed $v = 3.086$. When discretized under the sampling period 0.05 s, the system (43) has an unstable pole at $z = 1$, a common root of $D_1(z)$ and $D_2(z)$. However, the matrix $[N_1(1)^\top, N_2(1)^\top]^\top$ is invertible, satisfying condition 2) of Corollary 2. Thus, for any $N \geq l = 2$, the pair $(\mathcal{A}, \mathcal{B})$ from any data satisfying the condition (3) would be stabilizable.

As in Section III-D.2, we collected 10 pairs of u^d and y^d such that $\text{col}(u^d, y^d) \in \mathcal{W}_{100}$ and the condition (3) holds with respect to the data Hankel matrices for every $N \in [4, 16]$. The averaging method of Remark 5 is applied to each $Y_{f,i} H_i^\dagger$. With

fixed $Q = 100I_2$ and $R = I_2$, the controller (39) is obtained for each $N \in [4, 16]$.

Fig. 6 compares the performance of the controller (39) for different values of N , when $y(t)$ in (39) is replaced with $y(t) - y_{\text{ref}}$, where $y_{\text{ref}} = [10, 0]^\top$. The initial conditions were $x(0) = [0, 0, 15, 0]^\top$ and $\hat{x}(0) = [5, \dots, 5, 0_{(m+2)N}^\top]^\top \neq x(0)$, thus resulting in different responses by N in Fig. 6. To compare the transient responses clearly, neither online nor offline noise was considered, and it can be seen that the transient performance improves as N increases. Moreover, as depicted in Fig. 5, the \mathcal{H}_2 norm of (42) again tends to decrease as N increases.

Remark 7. The performance benefits of increasing the past input-output trajectory length N have also been discussed in the context of predictive control [4], [9], [32], [33]. However, when data-driven output feedback controllers are derived from non-minimal realizations such as (25), N has been set as the minimum [2], [11] or reduced afterwards [17], [18], in order to ensure the controllability of such realizations. Therefore, it is worth noting that our stability guarantee on the latent poles enables the increase of N for the class of systems specified in Corollary 2, which may lead to enhanced control performance as observed from the simulation results.

V. APPLICATION TO DATA-DRIVEN INVERSION

This section studies data-driven inversion, or unknown input estimation, which reconstructs the system's (previous) input from the output using input-output data matrices. Analogously to (1), existing data-driven inversion algorithms can be understood as data-driven representations of an L -delay inverse⁴ of the system, which also contain latent poles. We show that the stability of the latent poles can be guaranteed through the use of the Moore-Penrose inverse of the data matrix. This enables *asymptotic* input estimation for minimum-phase systems even under unknown initial input trajectory. We exploit this property to implement DD-DOB [21], which simultaneously estimates and rejects the input disturbance, without requiring knowledge of its initial trajectory in contrast to the method of [21].

We consider a SISO system whose relative degree $\nu \in \mathbb{Z}_{\geq 0}$ is unknown while its upper bound $\bar{\nu} \geq \nu$ is known. Besides $N \geq \bar{l}$, we introduce another parameter $L \in \mathbb{Z}_{\geq 0}$, satisfying $L \geq \bar{\nu}$ so that an L -delay inverse of the system always exists. To begin with, let us define the following set of trajectories.

Definition 2. For $k \in \mathbb{N}$ and $L \in \mathbb{Z}_{\geq 0}$, \mathcal{W}_k^L is defined by the set of $\text{col}(u, y)$ such that $u \in \mathbb{R}^k$ and $y \in \mathbb{R}^{k+L}$ satisfy $\text{col}(u, u', y) \in \mathcal{W}_{k+L}$ for some $u' \in \mathbb{R}^L$.

We construct data matrices so that each column of

$$\bar{H}_{\text{inv}} := \begin{bmatrix} U_p \\ U_f \\ Y_p \\ Y_f^L \end{bmatrix} \in \mathbb{R}^{(2N+L+2) \times T}$$

belongs to \mathcal{W}_{N+1}^L , where both U_p and Y_p have N rows, U_f is a row vector, and Y_f^L has $L+1$ rows. (Apart from this, we do

⁴A proper transfer function matrix $\hat{G}(z)$ is an L -delay inverse [34] of $G(z)$ if $\hat{G}(z)G(z) = \frac{1}{z^L}I_m$. An L -delay inverse of a SISO system always exists if L is greater than or equal to the relative degree.

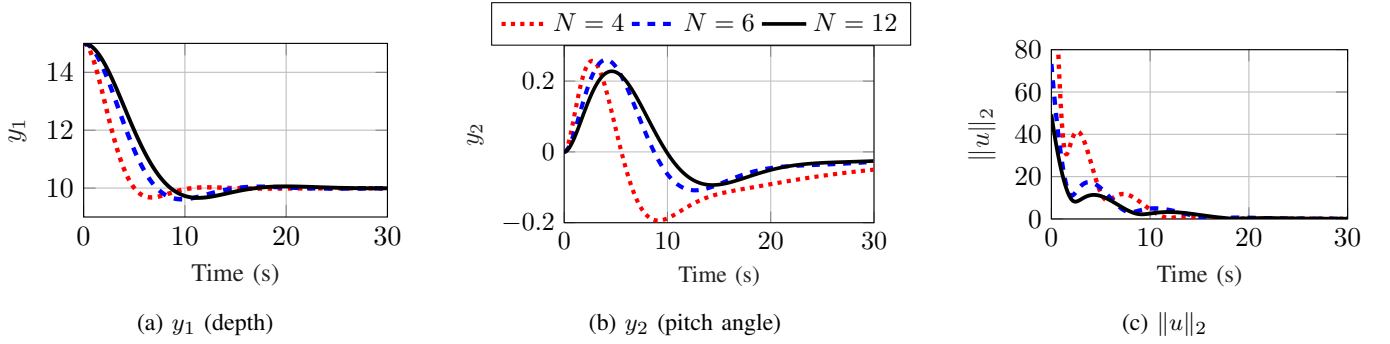


Fig. 6: Performance of the system (43) with the controller (39) by varying N .

not impose any specific structure on the data matrices unlike the previous works [20], [21].)

At time $t \in \mathbb{Z}_{\geq 0}$, the algorithm of [21] computes $\hat{u}(t-L)$, an estimate of the L -delayed input $u(t-L)$, as follows:

$$\hat{u}(t-L) = U_f g(t), \quad (44a)$$

where $g(t) \in \mathbb{R}^T$ is a solution to

$$H_{\text{inv}} g(t) := \begin{bmatrix} U_p \\ Y_p \\ Y_f^L \end{bmatrix} g(t) = \begin{bmatrix} \hat{u}(t-N-L:t-1-L) \\ y(t-N-L:t-1-L) \\ y(t-L:t) \end{bmatrix}, \quad (44b)$$

given the past N estimates and the system's (known) outputs. To begin with, we generalize the result of [21], showing that this estimation is correct under the condition

$$\text{rank}(H_{\text{inv}}) = N + n + L - \nu + 1 \quad (45)$$

and perfectly known initial input trajectory. To this end, we first present the following lemma.

Lemma 4. *Let $\text{col}(u^d, y^d) \in \mathcal{W}_k^L$ for $L \geq \nu$, $u^d \in \mathbb{R}^k$, and $y^d \in \mathbb{R}^{k+L}$. If u^d is persistently exciting of order $n+N+L+1$ with $N \geq l$ (i.e., $\mathcal{H}_{n+N+L+1}(u^d)$ has full row rank), then*

$$\text{rank} \left(\begin{bmatrix} \mathcal{H}_{N+1}(u^d) \\ \mathcal{H}_{N+L+1}(y^d) \end{bmatrix} \right) = N + n + L - \nu + 1. \quad (46)$$

Proof. See the Appendix III. \square

Lemma 4 provides a sufficient condition on the input data for satisfying (45) in case when $\bar{H}_{\text{inv}} = \begin{bmatrix} \mathcal{H}_{N+1}(u^d) \\ \mathcal{H}_{N+L+1}(y^d) \end{bmatrix}$; note that $\text{rank}(\bar{H}_{\text{inv}}) = \text{rank}(H_{\text{inv}})$ because U_f belongs to the row span of H_{inv} due to the existence of an L -delay inverse.

Based on Lemma 4, we show that (45) is a necessary and sufficient condition for \bar{H}_{inv} to fully characterize \mathcal{W}_{N+1}^L .

Proposition 4. *For $N \geq l$ and $L \geq \nu$, $\text{image } \bar{H}_{\text{inv}} = \mathcal{W}_{N+1}^L$ if and only if (45) holds. In this case, $\hat{u}(t-L) = u(t-L)$ for all $t \in \mathbb{Z}_{\geq 0}$ by (44) if $\hat{u}(t-L) = u(t-L)$ for all $t \in [-N, -1]$.*

Proof. By [21, Lemma 1], $\text{image } \begin{bmatrix} \mathcal{H}_{N+1}(u^d) \\ \mathcal{H}_{N+L+1}(y^d) \end{bmatrix} = \mathcal{W}_{N+1}^L$ for $\text{col}(u^d, y^d) \in \mathcal{W}_k^L$ where $u^d \in \mathbb{R}^k$ is persistently exciting of order $n+N+L+1$. Thus, $\dim(\mathcal{W}_{N+1}^L) = N+n+L-\nu+1$ by Lemma 4. Since $\text{image } \bar{H}_{\text{inv}} \subset \mathcal{W}_{N+1}^L$ as the system is LTI, $\text{image } \bar{H}_{\text{inv}} = \mathcal{W}_{N+1}^L$ if and only if (45) holds. The rest of the proof directly follows from [21, Theorem 2]. \square

Proposition 4 implies that \hat{u} in (44) can be replaced with u ; this makes (44) a data-driven representation of an L -delay inverse of the system, which is inherently recursive. To analyze the stability of (44), we rewrite (44) with respect to u as

$$u(t-L) = \eta^\top \begin{bmatrix} u(t-N-L:t-1-L) \\ y(t-N-L:t-1-L) \\ y(t-L:t) \end{bmatrix}, \quad (47)$$

with an arbitrary $\eta \in \mathbb{R}^{2N+L+1}$ such that $U_f = \eta^\top H_{\text{inv}}$. When applied the z -transform, (47) yields the transfer function of an L -delay inverse by Proposition 4 as

$$\frac{\delta_{N+L} z^{N+L} + \dots + \delta_1 z + \delta_0}{z^L (z^N - \gamma_{N-1} z^{N-1} - \dots - \gamma_0)} = \frac{D(z)}{z^L N(z)}, \quad (48)$$

where

$$\eta^\top = [\gamma_0, \gamma_1, \dots, \gamma_{N-1}, \delta_0, \delta_1, \dots, \delta_{N+L}]. \quad (49)$$

Then, it is clearly seen from (48) that the poles of (47) consist of the system's zeros, the origin, and $N-n+\nu$ latent poles.

We show that every latent pole in (47) is stable when $\eta^\top = U_f H_{\text{inv}}^\dagger$, or equivalently, when $g(t)$ of (44a) is chosen as the least-norm solution to (44b). We specifically write

$$U_f H_{\text{inv}}^\dagger = [c_0, c_1, \dots, c_{N-1}, d_0, d_1, \dots, d_{N+L}],$$

and define

$$N_{\text{inv}}^*(z) := z^N - \sum_{k=0}^{N-1} c_k z^k, \quad D_{\text{inv}}^*(z) := \sum_{k=0}^{N+L} d_k z^k.$$

Then, the following theorem states that only stable pole-zero cancellations occur in (47) when $\eta^\top = U_f H_{\text{inv}}^\dagger$.

Theorem 4. *Under the condition (45), there exists a Schur stable $C_{\text{inv}}^*(z) \in M_{N-n+\nu}$ such that*

$$N_{\text{inv}}^*(z) = \frac{1}{\rho} C_{\text{inv}}^*(z) N(z), \quad D_{\text{inv}}^*(z) = \frac{1}{\rho} C_{\text{inv}}^*(z) D(z), \quad (50)$$

where $\rho \in \mathbb{R}$ is the leading coefficient of $N(z)$. Furthermore, $C_{\text{inv}}^*(z)$ is determined solely by $G(z)$ and N .

Proof. By Proposition 4, the equality (48) holds for any $\eta \in \mathbb{R}^{2N+L+1}$ satisfying $U_f = \eta^\top H_{\text{inv}}$, which is parameterized as in (49). It follows that

$$z^N - \sum_{k=0}^{N-1} \gamma_k z^k = \frac{1}{\rho} C_{\text{inv}}(z) N(z), \quad \sum_{k=0}^{N+L} \delta_k z^k = \frac{1}{\rho} C_{\text{inv}}(z) D(z) \quad (51)$$

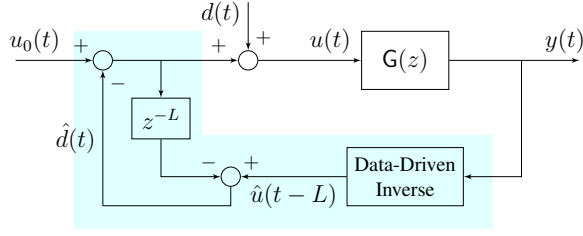


Fig. 7: Block diagram of a system with DD-DOB (the shaded area).

for some $C_{\text{inv}}(z) \in M_{N-n+\nu}$, since the polynomials $D(z)$ and $N(z)$ are relatively coprime. Conversely, as in Lemma 1, it is clear that given $C_{\text{inv}}(z) \in M_{N-n+\nu}$, the vector (49) defined by (51) satisfies $U_f = \eta^\top H_{\text{inv}}$. Thus, we define a function Ψ that maps η such that $U_f = \eta^\top H_{\text{inv}}$ to $C_{\text{inv}}(z)$ of (51), which is invertible. Then, (50) holds with $C_{\text{inv}}^*(z) = \Psi((U_f H_{\text{inv}}^\dagger)^\top)$. By the definition (13),

$$\begin{aligned} C_{\text{inv}}^*(z) &= \underset{C(z) \in M_{N-n+\nu}}{\operatorname{argmin}} \quad \|\Psi^{-1}(C(z))\|_2^2 \\ &= \underset{C(z) \in M_{N-n+\nu}}{\operatorname{argmin}} \quad f_{n-\nu, N-n+\nu} \left(C(z), \frac{1}{\rho} N(z), \frac{1}{\rho} D(z) \right), \end{aligned}$$

which implies that $C_{\text{inv}}^*(z)$ is determined solely by $G(z)$ and N . Moreover, by Lemma 3, $C_{\text{inv}}^*(z)$ is Schur stable. \square

Note that by Theorem 4, $d_{N+L} = \dots = d_{N+\nu+1} = 0$, that is, the degree of $D_{\text{inv}}^*(z)$ is $N + \nu$.

Theorem 4 also implies that when $\eta^\top = U_f H_{\text{inv}}^\dagger$, the data-driven inverse (47) is stable for minimum-phase systems, due to the stability of every latent pole. This enables asymptotic input estimation by (47), where the estimate $\hat{u}(t-L)$ asymptotically approaches the true input $u(t-L)$ despite an inaccurate initial estimate. This is shown by the following corollary.

Corollary 3. *Let $\hat{u}(t-L)$ be the L -delayed input estimate from (47) with $\eta^\top = U_f H_{\text{inv}}^\dagger$. Under the condition (45), $|u(t-L) - \hat{u}(t-L)| \rightarrow 0$ as $t \rightarrow \infty$ for any initial estimate $\hat{u}(-N-L : -1-L) \in \mathbb{R}^N$ if and only if the system is of minimum-phase.*

Proof. The proof directly comes from Theorem 4 and the fact that the dynamics of $e_u(t) := u(t-N-L : t-1-L) - \hat{u}(t-N-L : t-1-L)$ has eigenvalues at the zeros of the system and the roots of $C_{\text{inv}}^*(z)$. \square

Remark 8. *The method of [20] also aims to find an asymptotic unknown input estimator, which can be understood as finding a generalized inverse H_{inv}^G such that the dynamics of (47) with $\eta^\top = U_f H_{\text{inv}}^G$ is stable. However, it can be inferred from (48) that such H_{inv}^G does not exist for non-minimum phase systems, since (47) has unstable zeros of the system as its poles.*

A. Implementation of DD-DOB

The asymptotic property of Corollary 3 is particularly useful for DD-DOB [21]. Fig. 7 depicts the structure of DD-DOB, where $u_0(t)$ is the command input, $d(t)$ is the input additive disturbance, and $\hat{d}(t)$ is the estimated disturbance. As shown

in Fig. 7, $\hat{d}(t)$ is computed as

$$\begin{aligned} \hat{d}(t) &= \hat{u}(t-L) - (u_0(t-L) - \hat{d}(t-L)) \\ &= \hat{u}(t-L) - u(t-L) + d(t-L), \end{aligned}$$

so that

$$\begin{aligned} u(t) &= u_0(t) - (\hat{u}(t-L) - u(t-L)) \\ &\quad + (d(t) - d(t-L)). \end{aligned}$$

Then, when the disturbance is slowly varying as $d(t) \approx d(t-L)$, it is expected that its effect is approximately canceled, i.e., $u(t) \approx u_0(t)$.

Originally in [21], the data-driven inverse block of Fig. 7 is implemented as in (44), assuming that $\hat{u}(t-L) = u(t-L)$ for all $t \in [-N, -1]$, which requires perfect knowledge of the initial disturbance. In contrast, by employing (47) with $\eta^\top = U_f H_{\text{inv}}^\dagger$ as the inverse block, DD-DOB can operate properly without such an assumption for minimum-phase systems by Corollary 3. However, for non-minimum phase systems, (47) becomes unstable, which was also a problem for the original DD-DOB. Note that the minimum-phasesness is necessary for implementing the classical disturbance observer as well [29].

The effectiveness of DD-DOB using Corollary 3 is demonstrated by the simulation results depicted in Fig. 8. Here, the system is again (22) under the same setting as in Section III-D. The discretized system is of minimum-phase and $\nu = 1$. We constructed the data matrices with $(N, L, T) = (6, 2, 94)$, satisfying the condition (45). A disturbance $d(t) = 0.5 \sin(0.02t)$ is added to a step input $u_0(t)$, as shown in Fig. 8a. Compared to $u_0(t) + d(t)$, it can be seen from Fig. 8a that the disturbance is gradually removed from the actual input $u(t)$ by DD-DOB. Therefore, in Fig. 8b, the output $y(t)$ approaches $y_0(t)$, which refers to the output when there is no disturbance.

VI. CONCLUSION

We have studied the stability of the data-driven representation (1), focusing on the existence and stability of latent poles. It is shown that the stability of every latent pole is guaranteed by reformulating (1) into (7) using the Moore-Penrose inverses of the data matrices. We have also analyzed the effect of noise in data on (7), ensuring that the latent poles remain inside the stable region under sufficiently small noise.

The implications and applications of the main result have been extensively explored in the context of data-driven control and analysis. Due to the stability of the latent poles, applying the data-driven representation (7) recursively yields a stable output predictor if the underlying system is stable. Moreover, the latent poles become uncontrollable but stable modes of the state-space realization (25) constructed from (7), which can be applied to design data-driven output feedback controllers. As an example, we have designed a data-driven output feedback LQR controller, given the stabilizability of the realization (25). Finally, we have analyzed the stability of data-driven inverse, again showing that there are latent poles whose stability can be guaranteed through the use of the Moore-Penrose inverse of the data matrix. This enables asymptotic data-driven input estimation for minimum-phase systems when the initial input

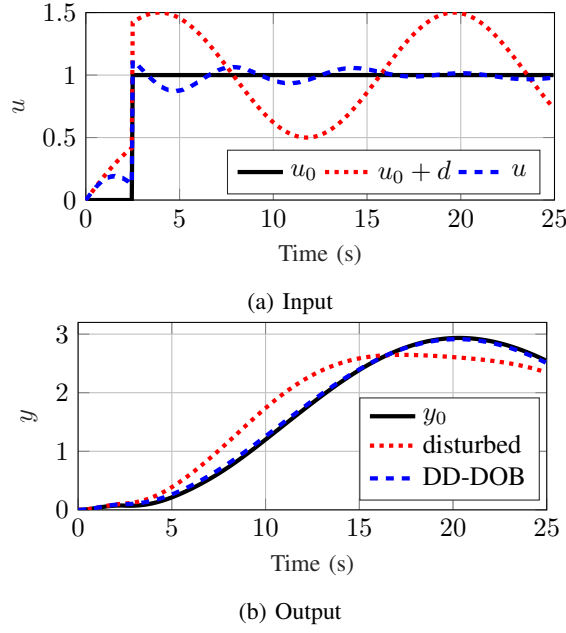


Fig. 8: Input and output of the system without disturbance (the black solid line), with disturbance (the red dotted line), and with both disturbance and DD-DOB (the blue dashed line).

trajectory is unknown; this property has been further utilized to implement DD-DOB.

Since our approach considers a multi-output system as a set of parallel single-output systems, more direct and fundamental approaches for multi-output systems remain to be explored. In addition, as the data-driven representation (7) for single-output systems is consistent with the subspace predictor [6] or the use of the projection-based regularizer [25], an interesting direction for future work would be to investigate the characteristics of latent poles generated by other types of regularizer. Another direction could be to analyze the effect of the past input-output trajectory length N on the realization (25) and on data-driven controllers synthesized from it.

APPENDIX I PROOF OF LEMMA 2

Let $p(z) = z^n + \sum_{k=0}^{n-1} p_k z^k$ and $q(z) = \sum_{k=0}^n q_k^\top z^k$. We define Toeplitz matrices for $p(z)$ and $q(z)$ by

$$(P_\tau, Q_\tau) := \left(\begin{bmatrix} 1 & 0 & 0 \\ p_{n-1} & 1 & 0 \\ p_{n-2} & p_{n-1} & 1 \\ p_{n-3} & p_{n-2} & p_{n-1} \\ \vdots & \vdots & \vdots \\ p_0 & p_1 & p_2 \\ 0 & p_0 & p_1 \\ 0 & 0 & p_0 \end{bmatrix}, \begin{bmatrix} q_n & 0_m & 0_m \\ q_{n-1} & q_n & 0_m \\ q_{n-2} & q_{n-1} & q_n \\ \vdots & \vdots & \vdots \\ q_0 & q_1 & q_2 \\ 0_m & q_0 & q_1 \\ 0_m & 0_m & q_0 \end{bmatrix} \right)$$

so that $P_\tau \in \mathbb{R}^{(n+3) \times 3}$ and $Q_\tau \in \mathbb{R}^{m(n+3) \times 3}$. We utilize the fact that multiplication of polynomials can be represented by a product between a Toeplitz matrix and a vector of coefficients. Specifically, for a polynomial $w(z) = w_2 z^2 + w_1 z + w_0$,

$$P_\tau \text{col}(w_2, w_1, w_0) = \text{col}(\bar{w}_{n+2}, \bar{w}_{n+1}, \dots, \bar{w}_0), \quad (52)$$

where \bar{w}_k is the k -th coefficient of $p(z)w(z)$. We also define

$$\begin{bmatrix} P_\tau^\top & Q_\tau^\top \end{bmatrix} \begin{bmatrix} P_\tau \\ Q_\tau \end{bmatrix} =: \begin{bmatrix} \theta_0 & \theta_1 & \theta_2 \\ \theta_1 & \theta_0 & \theta_1 \\ \theta_2 & \theta_1 & \theta_0 \end{bmatrix}.$$

We first prove 1). From the property (52), it follows that

$$\begin{aligned} f_{n,1}(z + \lambda, p(z), q(z)) &= \left\| \begin{bmatrix} P_\tau \\ Q_\tau \end{bmatrix} \begin{bmatrix} 0 \\ 1 \\ \lambda \end{bmatrix} \right\|_2^2 - 1 \\ &= \theta_0 \lambda^2 + 2\theta_1 \lambda + \theta_0 - 1, \end{aligned}$$

and thus $\lambda^* = -\theta_1/\theta_0$. By the Cauchy-Schwarz inequality,

$$|\theta_1| \leq \sqrt{\theta_0 - 1 - q_n^\top q_n} \sqrt{\theta_0 - p_0^2 - q_0^\top q_0} < \theta_0,$$

since

$$\begin{aligned} \theta_1 &= [p_{n-1}, p_{n-2}, \dots, p_0, q_{n-1}^\top, \dots, q_0^\top] \\ &\quad \cdot [1, p_{n-1}, \dots, p_1, q_n^\top, \dots, q_1^\top]^\top. \end{aligned}$$

Therefore, $|\lambda^*| < 1$, which concludes the proof of 1).

Next, we prove 2). It can be observed that

$$\begin{aligned} f_{n,2}(z^2 + \phi z + \psi, p(z), q(z)) &= \left\| \begin{bmatrix} P_\tau \\ Q_\tau \end{bmatrix} \begin{bmatrix} 1 \\ \phi \\ \psi \end{bmatrix} \right\|_2^2 - 1 \\ &= \theta_0 \phi^2 + \theta_0 \psi^2 + 2\theta_1 \phi \psi + 2\theta_1 \phi + 2\theta_2 \psi + \theta_0 - 1. \end{aligned} \quad (53)$$

Then, $[\phi^*, \psi^*]^\top$ is unique and $\psi^* = (\theta_1^2 - \theta_0 \theta_2)/(\theta_0^2 - \theta_1^2)$. Since $\theta_0^2 - \theta_1^2 > 0$, it suffices to show that $\theta_1^2 - \theta_0 \theta_2 < \theta_0^2 - \theta_1^2$. By substituting $\phi = -2\theta_1/\theta_0$ and $\psi = 1$ in (53), we have

$$\frac{1}{\theta_0} (2\theta_0^2 - 4\theta_1^2 + 2\theta_0 \theta_2 - \theta_0) \geq 0,$$

since the cost function is nonnegative by definition. As $\theta_0 \geq 1$ by definition, it follows that

$$\theta_0^2 - 2\theta_1^2 + \theta_0 \theta_2 \geq \frac{\theta_0}{2} \geq \frac{1}{2} > 0.$$

This concludes the proof.

APPENDIX II TECHNICAL LEMMA

Consider $A \in \mathbb{R}^{m \times n}$ and $b \in \mathbb{R}^m$ such that $b \in \text{image } A$. Let $r := \text{rank}(A) \leq l := \min\{m, n\}$. Suppose that A and b are both corrupted by noise matrices $E \in \mathbb{R}^{m \times n}$ and $e \in \mathbb{R}^m$, respectively, as

$$\tilde{A} := A + E, \quad \tilde{b} := b + e.$$

Generically, we assume that $\tilde{r} := \text{rank}(\tilde{A}) > r$. (If $\tilde{r} = r$, then $\tilde{A}^\dagger \rightarrow A^\dagger$ as $E \rightarrow 0_{m \times n}$ [26].) Let the singular values of A and \tilde{A} be σ_i and $\tilde{\sigma}_i$, respectively, where $\sigma_1 \geq \sigma_2 \geq \dots \geq \sigma_r > \sigma_{r+1} = \dots = \sigma_l = 0$ and $\tilde{\sigma}_1 \geq \tilde{\sigma}_2 \geq \dots \geq \tilde{\sigma}_{\tilde{r}} > \tilde{\sigma}_{\tilde{r}+1} = \dots = \tilde{\sigma}_l = 0$. Then, the following lemma holds.

Lemma 5. *If $0 < \tau < \sigma_r$, then for any $\epsilon > 0$, there exists $\delta > 0$ such that $\|A^\dagger b - [\tilde{A}^\dagger]^\dagger \tilde{b}\|_2 < \epsilon$ if $\|[E, e]\|_2 < \delta$.*

Proof. With the (compact) singular value decomposition, $A = U_0 \Lambda_0 V_0^\top$, where $U_0 \in \mathbb{R}^{m \times r}$ and $V_0 \in \mathbb{R}^{n \times r}$ have orthogonal

columns and $\Lambda_0 := \text{diag}(\sigma_1, \dots, \sigma_r)$. Note that by the Weyl's theorem, it can be shown that

$$|\sigma_i - \tilde{\sigma}_i| \leq \|E\|_2, \quad i \in \{1, \dots, l\}. \quad (54)$$

Therefore, for sufficiently small $\|E\|_2$, $\tau < \tilde{\sigma}_r$. Let $\kappa \in \mathbb{N}$ be such that $\tilde{\sigma}_\kappa > \tau \geq \tilde{\sigma}_{\kappa+1}$ (with $\tilde{\sigma}_{l+1} := 0$). Then, as $\kappa \geq r$,

$$\begin{aligned} \tilde{A} &= [\tilde{U}_0 \quad \tilde{U}_1 \quad \tilde{U}_2] \begin{bmatrix} \tilde{\Lambda}_0 & & \\ & \tilde{\Lambda}_1 & \\ & & \tilde{\Lambda}_2 \end{bmatrix} [\tilde{V}_0 \quad \tilde{V}_1 \quad \tilde{V}_2]^\top, \\ \tilde{\Lambda}_0 &:= \text{diag}(\tilde{\sigma}_1, \dots, \tilde{\sigma}_r), \quad \tilde{\Lambda}_1 := \text{diag}(\tilde{\sigma}_{r+1}, \dots, \tilde{\sigma}_\kappa), \\ \tilde{\Lambda}_2 &:= \text{diag}(\tilde{\sigma}_{\kappa+1}, \dots, \tilde{\sigma}_l) \in \mathbb{R}^{(m-\kappa) \times (n-\kappa)} \end{aligned}$$

by the singular value decomposition, where $[\tilde{U}_0, \tilde{U}_1, \tilde{U}_2]$ and $[\tilde{V}_0, \tilde{V}_1, \tilde{V}_2]$ are orthogonal. Thus, the rank- κ approximation of \tilde{A} becomes $\tilde{A}_\tau = \tilde{U}_0 \tilde{\Lambda}_0 \tilde{U}_0^\top + \tilde{U}_1 \tilde{\Lambda}_1 \tilde{U}_1^\top$. Since $b = A A^\dagger b + e$, it follows that

$$\begin{aligned} [\tilde{A}_\tau]^\dagger b &= \tilde{V}_0 \tilde{\Lambda}_0^{-1} \tilde{U}_0^\top U_0 \Lambda_0 V_0^\top A^\dagger b \\ &\quad + \tilde{V}_1 \tilde{\Lambda}_1^{-1} \tilde{U}_1^\top U_0 \Lambda_0 V_0^\top A^\dagger b + [\tilde{A}_\tau]^\dagger e. \end{aligned} \quad (55)$$

Since $1/\tilde{\sigma}_\kappa < 1/\tau$, both $\|[\tilde{A}_\tau]^\dagger\|_2$ and $\|\tilde{\Lambda}_1^{-1}\|_2$ are bounded by $1/\tau$. Then, $\|[\tilde{A}_\tau]^\dagger e\|_2 \rightarrow 0$ as $\|e\|_2 \rightarrow 0$. As $\|E\|_2 \rightarrow 0$, $\tilde{V}_0 \tilde{\Lambda}_0^{-1} \tilde{U}_0^\top \rightarrow A^\dagger$ because $\text{rank}(A) = \text{rank}(\tilde{U}_0 \tilde{\Lambda}_0 \tilde{U}_0^\top)$ (see [26]). Thus, the first term of (55) converges to $A^\dagger b$ as $\|E\|_2 \rightarrow 0$. Now it suffices to show that $\|\tilde{U}_1^\top U_0\|_2 \rightarrow 0$ as $\|E\|_2 \rightarrow 0$. We follow the proof of the Davis-Kahan theorem [35]. Let

$$H := \tilde{A} \tilde{A}^\top - A A^\top = E A^\top + A E^\top + E E^\top.$$

Since $\tilde{U}_1^\top \tilde{A} \tilde{A}^\top = \tilde{\Lambda}_1^2 \tilde{U}_1^\top$ and $A A^\top U_0 = U_0 \Lambda_0^2$, we have

$$\tilde{U}_1^\top H U_0 = \tilde{\Lambda}_1^2 \tilde{U}_1^\top U_0 - \tilde{U}_1^\top U_0 \Lambda_0^2.$$

Then, for any $c \in \mathbb{R}$,

$$\begin{aligned} \|\tilde{U}_1^\top H U_0\| &= \left\| \left(\tilde{\Lambda}_1^2 - c I_{\kappa-r} \right) \tilde{U}_1^\top U_0 - \tilde{U}_1^\top U_0 (\Lambda_0^2 - c I_r) \right\| \\ &\geq \left\| \left(\tilde{\Lambda}_1^2 - c I_{\kappa-r} \right) \tilde{U}_1^\top U_0 \right\| - \left\| \tilde{U}_1^\top U_0 (\Lambda_0^2 - c I_r) \right\|. \end{aligned}$$

Let $c \geq \|A\|_2^2$ so that by (54), $\tilde{\sigma}_{r+1}^2 < c$ with sufficiently small $\|E\|_2$. Then, we have

$$\begin{aligned} \|\tilde{U}_1^\top U_0\|_2 &\leq \left\| \left(\tilde{\Lambda}_1^2 - c I_{\kappa-r} \right)^{-1} \right\|_2 \left\| \left(\tilde{\Lambda}_1^2 - c I_{\kappa-r} \right) \tilde{U}_1^\top U_0 \right\|_2 \\ &\leq \frac{1}{c - \tilde{\sigma}_{r+1}^2} \left\| \left(\tilde{\Lambda}_1^2 - c I_{\kappa-r} \right) \tilde{U}_1^\top U_0 \right\|_2. \end{aligned}$$

In addition, it holds that

$$\left\| \tilde{U}_1^\top U_0 (\Lambda_0^2 - c I_r) \right\|_2 \leq (c - \sigma_r^2) \left\| \tilde{U}_1^\top U_0 \right\|_2.$$

With sufficiently small $\|E\|_2$, $\sigma_r > \tilde{\sigma}_{r+1}$ by (54), and thus

$$\left\| \tilde{U}_1^\top U_0 \right\|_2 \leq \frac{1}{\sigma_r^2 - \tilde{\sigma}_{r+1}^2} \left\| \tilde{U}_1^\top H U_0 \right\|_2.$$

Since $\|H\|_2 \rightarrow 0$ as $\|E\|_2 \rightarrow 0$, the proof is concluded. \square

APPENDIX III PROOF OF LEMMA 4

Let $\bar{H}_{\text{inv}} = \begin{bmatrix} \mathcal{H}_{N+1}(u^d) \\ \mathcal{H}_{N+L+1}(y^d) \end{bmatrix}$. Since U_f belongs to the row span of \bar{H}_{inv} , we show that (45) holds. By Definition 2, there exists $\bar{u}^d \in \mathbb{R}^L$ such that $\text{col}(u^d, \bar{u}^d, y^d) \in \mathcal{W}_{k+L}$. It is clear that $\text{col}(u^d, \bar{u}^d)$ is also persistently exciting of order $n + N + L + 1$, due to the Hankel structure. Let us consider a minimal realization $(\bar{A}, \bar{B}, \bar{C}, \bar{D})$ and the corresponding (virtual) state trajectory $x^d \in \mathbb{R}^{n(k-N)}$ that yields $\text{col}(u^d, y^d)$. The matrix

$$\begin{bmatrix} U_p \\ U_f^L \\ X \end{bmatrix} := \begin{bmatrix} \mathcal{H}_{N+L+1}(\text{col}(u^d, \bar{u}^d)) \\ \mathcal{H}_1(x^d) \end{bmatrix}$$

has full row rank by [7, Corollary 2], where U_f^L and X have $L + 1$ and n rows, respectively. For $i \in \mathbb{N}$, we define

$$\mathcal{O}_i := \begin{bmatrix} \bar{C} \\ \bar{C} \bar{A} \\ \vdots \\ \bar{C} \bar{A}^{i-1} \end{bmatrix}, \quad \mathcal{T}_i := \begin{bmatrix} \bar{D} & 0 & \cdots & 0 \\ \bar{C} \bar{B} & \bar{D} & & \\ \vdots & \vdots & \ddots & \vdots \\ \bar{C} \bar{A}^{i-1} \bar{B} & \bar{C} \bar{A}^{i-2} \bar{B} & \cdots & \bar{D} \end{bmatrix},$$

and $\mathcal{T}_0 := \bar{D}$. Then,

$$\begin{bmatrix} Y_p \\ Y_f^L \end{bmatrix} = \mathcal{O}_{N+L+1} X + \mathcal{T}_{N+L} \begin{bmatrix} U_p \\ U_f^L \end{bmatrix},$$

and by the structure of \mathcal{T}_{N+L} and \mathcal{O}_{N+L+1} ,

$$H_{\text{inv}} = \begin{bmatrix} U_p \\ Y_p \\ Y_f^L \end{bmatrix} = \begin{bmatrix} I_N & 0_{N \times (L+1)} & 0_{N \times n} \\ * & 0_{N \times (L+1)} & \mathcal{O}_N \\ * & \mathcal{T}_L & * \end{bmatrix} \begin{bmatrix} U_p \\ U_f^L \\ X \end{bmatrix}.$$

It can be seen that $\text{rank}(H_{\text{inv}}) = N + \text{rank}(\mathcal{T}_L) + \text{rank}(\mathcal{O}_N)$. As $N \geq l$, $\text{rank}(\mathcal{O}_N) = n$. By [34], $\text{rank}(\mathcal{T}_i) - \text{rank}(\mathcal{T}_{i-1}) = 1$ ($\text{rank}(\mathcal{T}_{-1}) := 0$) if and only if $i \geq \nu$, and thus $\text{rank}(\mathcal{T}_L) = L - \nu + 1$. This concludes the proof.

REFERENCES

- [1] J. Coulson, J. Lygeros, and F. Dörfler, "Data-enabled predictive control: In the shallows of the DeePC," in *Eur. Control Conf.*, 2019, pp. 307–312.
- [2] C. De Persis and P. Tesi, "Formulas for data-driven control: Stabilization, optimality, and robustness," *IEEE Trans. Autom. Control*, vol. 65, no. 3, pp. 909–924, 2020.
- [3] H. J. van Waarde, J. Eising, H. L. Trentelman, and M. K. Camlibel, "Data informativity: A new perspective on data-driven analysis and control," *IEEE Trans. Autom. Control*, vol. 65, no. 11, pp. 4753–4768, 2020.
- [4] I. Markovsky, L. Huang, and F. Dörfler, "Data-driven control based on the behavioral approach: From theory to applications in power systems," *IEEE Control Syst. Mag.*, vol. 43, no. 5, pp. 28–68, 2023.
- [5] I. Markovsky, J. C. Willems, P. Rapisarda, and B. L. M. De Moor, "Algorithms for deterministic balanced subspace identification," *Automatica*, vol. 41, no. 5, pp. 755–766, 2005.
- [6] W. Favoreel, B. L. M. De Moor, and M. Gevers, "SPC: Subspace predictive control," *IFAC Proc. Vol.*, vol. 32, no. 2, pp. 4004–4009, 1999.
- [7] J. C. Willems, P. Rapisarda, I. Markovsky, and B. L. M. De Moor, "A note on persistency of excitation," *Syst. Control Lett.*, vol. 54, no. 4, pp. 325–329, 2005.
- [8] I. Markovsky and P. Rapisarda, "Data-driven simulation and control," *Int. J. Control*, vol. 81, no. 12, pp. 1946–1959, 2008.
- [9] I. Markovsky and F. Dörfler, "Behavioral systems theory in data-driven analysis, signal processing, and control," *Annu. Rev. Control*, vol. 52, pp. 42–64, 2021.
- [10] —, "Identifiability in the behavioral setting," *IEEE Trans. Autom. Control*, vol. 68, no. 3, pp. 1667–1677, 2023.

- [11] X. Dai, C. De Persis, and N. Monshizadeh, "Data-driven optimal output feedback control of linear systems from input-output data," *IFAC-PapersOnLine*, vol. 56, no. 2, pp. 1376–1381, 2023.
- [12] J. Berberich, C. W. Scherer, and F. Allgöwer, "Combining prior knowledge and data for robust controller design," *IEEE Trans. Autom. Control*, vol. 68, no. 8, pp. 4618–4633, 2023.
- [13] J. Berberich, J. Köhler, M. A. Müller, and F. Allgöwer, "On the design of terminal ingredients for data-driven MPC," *IFAC-PapersOnLine*, vol. 54, no. 6, pp. 257–263, 2021.
- [14] L. Li, A. Bisoffi, C. De Persis, and N. Monshizadeh, "Controller synthesis from noisy-input noisy-output data," *Automatica*, vol. 183, 2026, Art. no. 112545.
- [15] B. Gopinath, "On the identification of linear time-invariant systems from input-output data," *Bell Syst. Tech. J.*, vol. 48, no. 5, pp. 1101–1113, 1969.
- [16] M. Budin, "Minimal realization of discrete linear systems from input-output observations," *IEEE Trans. Autom. Control*, vol. 16, no. 5, pp. 395–401, 1971.
- [17] M. Alsalti, V. G. Lopez, and M. A. Müller, "Notes on data-driven output-feedback control of linear MIMO systems," *IEEE Trans. Autom. Control*, vol. 70, no. 9, pp. 6143–6150, 2025.
- [18] R. S. Smith, M. Abdalmoaty, and M. Yin, "Data-driven formulation of the Kalman filter and its application to predictive control," in *Conf. Decision Control*, 2024, pp. 2633–2639.
- [19] M. K. Camlibel, H. J. van Waarde, and P. Rapisarda, "The shortest experiment for linear system identification," *Syst. Control Lett.*, vol. 197, 2025, Art. no. 106045.
- [20] J. Shi, Y. Lian, and C. N. Jones, "Data-driven input reconstruction and experimental validation," *IEEE Control Syst. Lett.*, vol. 6, pp. 3259–3264, 2022.
- [21] Y. Eun, J. Lee, and H. Shim, "Data-driven inverse of linear systems and application to disturbance observers," in *Am. Control Conf.*, 2023, pp. 2806–2811.
- [22] Y. Pedari, J. Lee, Y. Eun, and H. Ossareh, "Data-driven system interconnections and a novel data-enabled internal model control," in *Am. Control Conf.*, 2024, pp. 4326–4332.
- [23] J. Coulson, J. Lygeros, and F. Dörfler, "Distributionally robust chance constrained data-enabled predictive control," *IEEE Trans. Autom. Control*, vol. 67, no. 7, pp. 3289–3304, 2022.
- [24] H. J. van Waarde, C. De Persis, M. K. Camlibel, and P. Tesi, "Willems' fundamental lemma for state-space systems and its extension to multiple datasets," *IEEE Control Syst. Lett.*, vol. 4, no. 3, pp. 602–607, 2020.
- [25] F. Dörfler, J. Coulson, and I. Markovsky, "Bridging direct and indirect data-driven control formulations via regularizations and relaxations," *IEEE Trans. Autom. Control*, vol. 68, no. 2, pp. 883–897, 2023.
- [26] G. W. Stewart, "On the continuity of the generalized inverse," *SIAM J. Appl. Math.*, vol. 17, no. 1, pp. 33–45, 1969.
- [27] I. Markovsky, "A software package for system identification in the behavioral setting," *Control Eng. Pract.*, vol. 21, no. 10, pp. 1422–1436, 2013.
- [28] G. F. Franklin, J. D. Powell, and A. Emami-Naeini, *Feedback Control of Dynamic Systems*. Pearson, 2019.
- [29] H. Shim and N. H. Jo, "An almost necessary and sufficient condition for robust stability of closed-loop systems with disturbance observer," *Automatica*, vol. 45, no. 1, pp. 296–299, 2009.
- [30] F. L. Lewis, D. Vrabie, and V. L. Syrmos, *Optimal control*. John Wiley & Sons, 2012.
- [31] E. Liceaga-Castro and G. M. van der Molen, "Submarine H^∞ depth control under wave disturbances," *IEEE Trans. Control Syst. Technol.*, vol. 3, no. 3, pp. 338–346, 1995.
- [32] V. Breschi, A. Chiuso, and S. Formentin, "Data-driven predictive control in a stochastic setting: a unified framework," *Automatica*, vol. 152, 2023, Art. no. 110961.
- [33] N. H. Jo, H. Shim, and J. Lee, "Non-minimal input-output representation and its application to model predictive control," 2025, under review.
- [34] M. Sain and J. Massey, "Invertibility of linear time-invariant dynamical systems," *IEEE Trans. Autom. Control*, vol. 14, no. 2, pp. 141–149, 1969.
- [35] C. Davis and W. M. Kahan, "The rotation of eigenvectors by a perturbation. III," *SIAM J. Numer. Anal.*, vol. 7, no. 1, pp. 1–46, 1970.



Joowon Lee (Graduate Student Member, IEEE) received the B.S. degree in electrical and computer engineering in 2019, from Seoul National University, South Korea. She is currently a combined M.S./Ph.D. student in electrical and computer engineering at Seoul National University, South Korea. Her research interests include data-driven control, encrypted control systems, and security of cyber-physical systems.



Nam Hoon Jo (Member, IEEE) received the B.S., M.S., and Ph.D. degrees all from Electrical Engineering, Seoul National University, Seoul, South Korea, in 1992, 1994, and 2000, respectively. From 2000 to 2001, he was a Post-doctoral Research Associate at Automation and Systems Research Institute (ASRI) at Seoul National University, Seoul, Korea. From 2001 to 2002, he worked as a Senior Research Engineer at Samsung Electronics, Suwon, Korea. Since 2002, he has been with the School of Electrical Engineering at Soongsil University, Seoul, Korea, where he is currently a professor. His research interests include nonlinear systems control theory, disturbance observer, and data driven control.



Hyungbo Shim (Senior Member, IEEE) received the B.S., M.S., and Ph.D. degrees from Seoul National University, Korea, and held the post-doc position at University of California, Santa Barbara till 2001. He joined Hanyang University, Seoul, in 2002. Since 2003, he has been with Seoul National University, Korea. He served as associate editor for *Automatica*, *IEEE Transactions on Automatic Control*, *Int. Journal of Robust and Nonlinear Control*, and *European Journal of Control*, and as editor for *Int. Journal of Control, Automation, and Systems*. His research interests include stability analysis of nonlinear systems, observer design, disturbance observer technique, secure control systems, and synchronization for multi-agent systems.



Florian Dörfler (Senior Member, IEEE) is a Professor at the Automatic Control Laboratory at ETH Zürich. He received his Ph.D. degree in Mechanical Engineering from the University of California at Santa Barbara in 2013, and a Diplom degree in Engineering Cybernetics from the University of Stuttgart in 2008. From 2013 to 2014 he was an Assistant Professor at the University of California Los Angeles. He has been serving as the Associate Head of the ETH Zürich Department of Information Technology and Electrical Engineering from 2021 until 2022. His research interests are centered around automatic control, system theory, optimization, and learning. His particular foci are on network systems, data-driven settings, and applications to power systems. He is a recipient of the 2025 Rössler Prize, the highest scientific award at ETH Zürich across all disciplines, as well as the distinguished career awards by IFAC (Manfred Thoma Medal 2020) and EUCA (European Control Award 2020). He and his team received best paper distinctions in the top venues of control, machine learning, power systems, power electronics, circuits and systems.



Jinsung Kim (Member, IEEE) received Ph.D. degree in mechanical engineering from the Korea Advanced Institute of Science and Technology (KAIST), Daejeon, South Korea, in 2013. He is currently a Part Leader and Senior Research Engineer at the Vehicle Control Development Center, Hyundai Motor Company, Hwaseong, South Korea, where he has been since 2013. His previous works include control and estimation algorithm for dual clutch transmissions and model predictive control for gasoline engines in mass production vehicles. From 2019 to 2020, he was a Visiting Scholar with the University of Pennsylvania, Philadelphia, PA, USA. His current research interests include learning-based control, and vehicle motion control based on software-defined vehicle platform.